2016

Extensive Sensitivity Analysis and Parallel Stochastic Global Optimization Using Radial Basis Functions of Integrated Biorefineries under Operational Level Uncertainties

Santiago David Salas Ortiz
Louisiana State University and Agricultural and Mechanical College, ssalas3@lsu.edu

EXTENSIVE SENSITIVITY ANALYSIS AND PARALLEL STOCHASTIC GLOBAL OPTIMIZATION USING RADIAL BASIS FUNCTIONS OF INTEGRATED BIOREFINERIES UNDER OPERATIONAL LEVEL UNCERTAINTIES

A Thesis

Submitted to the Graduate Faculty of the
Louisiana State University and
Agricultural and Mechanical College
in partial fulfillment of the
requirements for the degree of
Master of Science

in

The Cain Department of Chemical Engineering

by
Santiago David Salas Ortiz
B.S., Universidad Central del Ecuador, 2012
May 2016

To God, *Regina Immaculata*, family and friends.

ACKNOWLEDGEMENTS

I would like to express my gratitude to my adviser Dr. José A. Romagnoli for his guidance and encouragement in my research. Moreover, to the members of my exam committee, Dr. John Flake, Dr. Francisco Hung and Dr. Warren T. Liao for their help in reviewing and evaluating my research. Also, to Dr. Aryan Geraili for introducing me to the topic of biorefineries optimization, and explaining me the process simulation and preliminary optimization algorithms. Finally, to PSE at LSU for their support, friendship and cordiality, especially to Jorge Chebeir MSc. who motivated me during hard times and became an example of hard working and determination.

I would like to thank to my beloved ones who supported me during this process. Marco Antonio, Gina and Paula Cristina, many thanks for being an awesome family. Also, my grandma and aunts, especially Soraya who almost every day sent me motivational messages for continuing in the battle. Finally, in memory of my grandmother Luz B. Palacios. Love y'all.

My special acknowledge to Fulbright Commission for honoring me with the scholarship that made this dream possible, and the Louisiana State University's Cain Department of Chemical Engineering for opening me their doors.

TABLE OF CONTENTS

LIST OF TABLES

LIST OF FIGURES

NOMENCLATURE

Indices	
$f = 1, \ldots, F$	Decision variables.
$g = 1, \ldots, G$	Number of expensive function simulations.
$h = 1, \ldots, H$	Number of uncertain parameters.
$i = 1, \ldots, D$	Times a population of uncertain parameters is generated.
$j = 1, \ldots, J$	RBF evaluated points.
$n = 1, \ldots, N$	Number of samples per parameter in sensitivity analysis.
$p = 1, \ldots, P$	Processors/workers.
$q = 1, \ldots, Q$	Number of parameters evaluated in sensitivity analysis.

Parameters	
EHCF	Simultaneous hydrolysis and co-fermentation for ethanol production
α	relating substrate reactivity with degree of hydrolysis
E1max	maximum enzyme 1 that can be adsorbed on substrate
E2max	maximum enzyme 2 that can be adsorbed on substrate
K1ad	dissociation constant for enzyme 1
K2ad	dissociation constant for enzyme 2
K1r	reaction rate constant 1
K1IG2	inhibition constant for cellobiose 1
K1IG	inhibition constant for glucose 1
K1IXy	inhibition constant for xylose 1
K2r	reaction rate constant 2
K2IG2	inhibition constant for cellobiose 2
K2IG	inhibition constant for glucose 2
K2IXy	inhibition constant for xylose 2
K3r	reaction rate constant 3
K3M	substrate (cellobiose) saturation constant
K3IG	inhibition constant for glucose 3
K3IXy	inhibition constant for xylose 3
Ea	activation energy
$\mu m_{,g}$	maximum specific growth rate in cell growth (glucose as substrate)
K4g	monod constant for growth on glucose
K4Ig	inhibition constant for growth on glucose
$CEtmax_{,g}$	maximum ethanol concentration in cell growth (glucose as substrate)
$CEtx_{,g}$	threshold Ethanol Concentration in cell growth (glucose as substrate)
$\mu m_{,xy}$	maximum specific growth rate in cell growth (xylose as substrate)
K5xy	monod constant for growth on glucose
K5Ixy	inhibition constant for growth on xylose
$CEtmax_{,xy}$	maximum ethanol concentration in cell growth (xylose as substrate)

$CEtx_{,xy}$	threshold Ethanol Concentration in cell growth (xylose as substrate)
α	weighing factor for glucose consumption
$qsmax,g$	overall maximum specific glucose utilization
$K7g$	substrate limitation constant in glucose consumption
$K7Isg$	substrate Inhibition constant in glucose consumption
$CEtis_{,g}$	threshold Ethanol Concentration in glucose consumption
$CEtmax_{,g}$	maximum ethanol concentration in glucose consumption
$qsmax,xy$	overall maximum specific xylose utilization
$K8xy$	substrate limitation constant
$K8Isxy$	substrate Inhibition constant in xylose consumption
$CEtis_{,xy}$	threshold Ethanol Concentration in xylose consumption
$CEtmaxsxy$	maximum ethanol concentration in xylose consumption
$qpmax,g$	overall maximum specific ethanol production by glucose fermentation
$K9g$	substrate limitation constant in glucose fermentation
$K9Ipg$	substrate Inhibition constant in glucose fermentation
$CEtip_{,g}$	threshold Ethanol Concentration in glucose fermentation
$CEtimaxp_{,g}$	maximum ethanol concentration in glucose fermentation
$qpmax,xy$	overall maximum specific ethanol production by xylose fermentation
$K10xy$	substrate limitation constant in xylose fermentation
$K10Ipxy$	substrate Inhibition constant in xylose fermentation
$CEtip_{,xy}$	threshold Ethanol Concentration in xylose fermentation
$CEtmaxp_{,xy}$	maximum ethanol concentration in xylose fermentation
SAEH	Enzymatic hydrolysis for succinic acid production
αsa	relating substrate reactivity with degree of hydrolysis
$E1max_{sa}$	maximum enzyme 1 that can be adsorbed on substrate
$E2max_{sa}$	maximum enzyme 2 that can be adsorbed on substrate
$K1ad_{sa}$	dissociation constant for enzyme 1
$K2ad_{sa}$	dissociation constant for enzyme 2
$K1r_{sa}$	reaction rate constant 1
$K1IG2_{sa}$	inhibition constant for cellobiose 1
$K1IG_{sa}$	inhibition constant for glucose 1
$K1IXy_{sa}$	inhibition constant for xylose 1
$K2r_{sa}$	reaction rate constant 2
$K2IG2_{sa}$	inhibition constant for cellobiose 2
$K2IG_{sa}$	inhibition constant for glucose 2
$K2IXy_{sa}$	inhibition constant for xylose 2
$K3r_{sa}$	reaction rate constant 3
$K3M_{sa}$	substrate (cellobiose) saturation constant
$K3IG_{sa}$	inhibition constant for glucose 3
$K3IXy_{sa}$	inhibition constant for xylose 3
Ea_{sa}	activation energy
SACF	Co-fermentation for succinic acid production
$\mu m_{,sg}$	maximum specific growth rate in glucose fermentation
KSg	glucose saturation constant

$KSIg$	inhibition constant for growth on glucose
$PCrit_{,g}$	critical product concentration at which cell growth fully stops
i	degree of product inhibition
Kd	specific death rate
Yi	stoichiometric yield coefficient of cell on glucose
YSA	stoichiometric yield coefficient of succinic acid on glucose
YAA	stoichiometric yield coefficient of acetic acid on glucose
YFA	stoichiometric yield coefficient of formic acid on glucose
YLA	stoichiometric yield coefficient of lactic acid on glucose
msg	specific maintenance coefficient
αSA	growth-associated parameter for succinic acid formation
βSA	non-growth-associated parameter for succinic acid formation
αAA	growth-associated parameter for acetic acid formation
βAA	non-growth-associated parameter for acetic acid formation
αFA	growth-associated parameter for formic acid formation
βFA	non-growth-associated parameter for formic acid formation
βLA	non-growth-associated parameter for lactic acid formation

ABSTRACT

This work presents a decision-making framework for global optimization of detailed renewable energy processes considering technological uncertainty. The critical uncertain sources are identified with an efficient computational method for global sensitivity analysis, and are obtained in two different ways, simultaneously and independently per product pathway respect to the objective function. For global optimization, the parallel stochastic response surface method developed by Regis & Shoemaker (2009) is employed. This algorithm is based on the multi-start local metric stochastic response surface method explored by the same authors (2007a). The aforementioned algorithm uses as response surface model a radial basis function (RBF) for approximating the expensive simulation model. Once the RBF's parameters are fitted, the algorithm selects multiple points to be evaluated simultaneously. The next point(s) to be evaluated in the expensive simulation are obtained based on their probability to attain a better result for the objective function. This approach represents a simplified oriented search. To evaluate the efficacy of this novel decision-making framework, a hypothetical multiproduct lignocellulosic biorefinery is globally optimized on its operational level. The obtained optimal points are compared with traditional optimization methods, e.g. Monte-Carlo simulation, and are evaluated for both proposed types of uncertainty calculated.

1. INTRODUCTION

Propped by worldwide population and industry growth, it is estimated that by 2040 the global energy consumption will merge in 56%, from 524 quadrillion of British thermal units (Btu) to 820 quadrillion Btu (EIA, 2013). Currently, around 85% of world's energy comes from fossil fuel resources. In the U.S., approximately 79% of energy sources come from non-renewables, making it the highest share of the energy sources in the market. Figure 1 shows the share per energy sector in the United States in 2013 (Dale & Holtzapple, 2015). Even though in the past year the price of oil has been dropping from its previous attractive peak, its volatility and uncertainty should encourage governments to diversify theirs energy portfolios. Cheap oil prices should not be a temptation for stepping away from renewables. Indeed, uncertainty and variability of oil in the market shall encourage investors, shareholders and decision-makers to prepare for the long farewell that mankind has to say to fossil fuels.

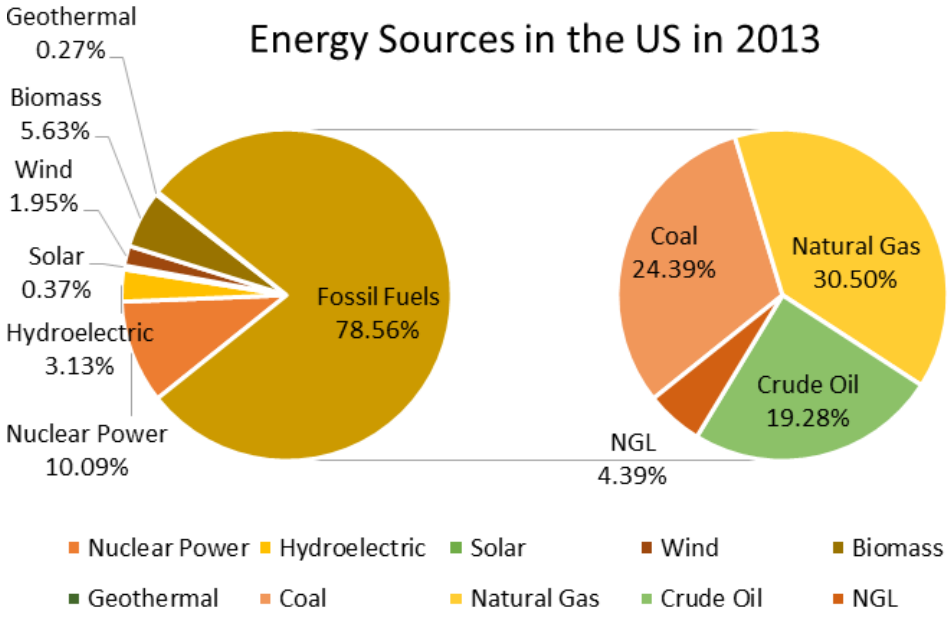

Figure 1: Energy surces in the US 2013

Many efforts have been done in order to promote renewable energy sources as global population recognizes being dependent on limited resources, such as fossil fuels. The modern portfolio of available renewables includes biofuels produced from biomass, which appears to be a sustainable and reasonable solution for mobile energy services giving also an innovative usage of organic waste. However, market volatility, technological uncertainty, and limited experience in biorefining processes can prevent the development of this burgeoning industry.

By processing biomass, e.g., lignocellulose, in mainly biochemical or thermochemical pathways, industrial biorefineries are able to produce fuels, heat, bioelectricity, and value-added chemicals. First and second generation biorefineries are already operating worldwide and are expected to foment economic growth and reduce mineral oil dependency (Kokossis et al., 2015). Process systems engineering has contributed over the past few years in addressing the complexity of the decision-making and modeling problem in order to optimize and make cost-effective renewable energy projects. The regular approach to optimize these type of processes considers most of the time a deterministic design approach (Geraili et al., 2014; Martín & Grossmann, 2011; Leduc et al., 2010; Zhang et al., 2013; Zondervan et al., 2011), in which the model assumes that all the parameters are known from experimental data. By assuming ideality, external factors that might affect the process behavior and the project profitability are neglected. However, during the conceptual design of a project there is lack of information at different levels which generates uncertainty. The global optimization problem should be addressed considering risk management at the technological level in conceptual stages. Thus, decision-makers can have a versatile approach for making and supporting critical decisions.

When processes are in their first stages, they appear to be uncertain for managers and investors. Lack of understanding and, more important, experience with new technologies can harm the

economy of a renewable energy enterprise. In order to minimize risk and maximize the success of a biorefinery endeavor, it is required to measure uncertainties from the process and anticipate their effect. In other words, it is imperative to develop a technological risk management strategy able to provide a low risk solution of the problem. Uncertainties at the operational level are multiple and can be found in various parts. The lack of experience when scaling-up new equipment can be a source. Parameters that explain chemical reactions and are obtained considering probability distributions, and limited thermodynamic data of complex or non-studied chemical species contribute to uncertainty as well. To underestimate these limitations may lead into non-optimal designs and even generate extra expenses or difficulties during startup and operation. A typical form to estimate uncertainties is by applying a sensitivity analysis (Sobol', 1993; Saltelli, 2002; Wu et al, 2011). Literature review presents studies which aforethought integrated biorefinery optimization under price, supply chain, demand and operational level uncertainties (Dal-Mas et al., 2011; Kim et al., 2011; Kostin et al., 2012; Morales-Rodriguez et al, 2012) respectively. The optimization strategies available in literature trend to reduce the complexity of the problem into a mixed integer linear programming (MILP), or perform stochastic optimization methods such as Monte-Carlo simulations. Other optimization strategies are usually non feasible due to the computational cost of the simulation model when uncertainties are considered.

Surrogate models, also known as response surface or meta-models, are approximations of expensive functions. Since surrogate models have the capability of simplifying highly non-linear problems, they are widely utilized in multi-objective optimization (Simpson, 2001). Literature shows that metamodelling optimization strategies have applications in diverse fields of engineering (Razavi et al., 2012). Some relevant studies include, groundwater systems analysis and modeling including uncertainties (Keating et al., 2010; Mugunthan & Shoemaker, 2006;

Zhang et al., 2009; Zou et al., 2009), optimization problems that study groundwater bioremediation (Regis & Shoemaker, 2004; Regis & Shoemaker, 2007a; Regis & Shoemaker, 2007b; Regis & Shoemaker, 2009), and in aviation environmental systems modeling for uncertainty estimation (Allaire & Willcox, 2010).

In a previous work (Geraili & Romagnoli, 2015), proposed a systematic optimization methodology for biorefining processes under uncertainties. Also, as an improvement of this framework an optimal design considering both, strategic and operational level uncertainties was explored (Geraili et al., 2016). The present work continues this proposed idea and aims to explore deeply in uncertainty sources while optimizing the process variables of a renewable energy endeavor employing a novel methodology. In Chapter 2 the framework for expensive model-based processes optimization under uncertainty is presented, and the multi-product biorefinery model is explained. In Chapter 3 two sensitivity analysis approaches are presented, the first one when sensitivity indices are calculated simultaneously and the other one when sensitivity indices are calculated independently per product pathway. In Chapter 4 the objective function to be optimized is defined, and the optimization method is presented and explained. For global optimization, the parallel version of the multi-start local metric stochastic response surface method with restart, developed and tested by Regis & Shoemaker (2009), is employed. The surrogate model selects the next evaluation point(s) based on the proximity to previously selected and evaluated ones and by exploring the fitted RBF. Parallel computing of the expensive function can be done on multiple processors. In Chapter 5 the optimal points founds are tested and statistically evaluated with other points obtained using conventional methods, e.g. Monte-Carlo simulation. Finally, Chapter 6 presents general conclusions and provide future work in the field.

Information regarding the publications and presentations from this research work are listed below:

Publications

- "A Decision Support Tool for Optimal Design of Integrated Biorefineries under Strategic and Operational Level Uncertainties", *Industrial & Engineering Chemistry Research*, 2016, Vol. 55, Pages: 1667-1676.
- "Extensive Sensitivity Analysis and Parallel Stochastic Global Optimization Using Radial Basis Functions of Renewable Energy Businesses under Operational Level Uncertainties", under review.

Conference presentations

- "Scheme for multi-objective optimization in the design of integrated biorefineries under uncertainty"

  21st Latin-American Chemical Engineering Student Conference, Antigua, Guatemala (2015).

2. A FRAMEWORK FOR OPTIMIZATION OF EXPENSIVE MODEL-BASED PROCESSES UNDER UNCERTAINTY

2.1 Literature Review

Different optimization frameworks have been developed recently for optimizing renewable energy processes under different types and levels of uncertainty. For instance, optimization under uncertainties in biomass costs and biofuels' prices have been addressed previously by Dal-Mas et al. (2011), who concluded that in some scenarios the most adequate solution is to not enter in the business. Moreover, logistics and supply chain seem to be an important constraint for critical decision-making in a renewable energy business. Candidate sites, capacities, supply chain locations and quantities have been studied under uncertainty represented over different scenarios. The optimization problem was simplified into a two stage mixed integer stochastic programming platform able to define the size and location of the facility, and the input and output flows in order to select the most profitable scenario using Monte-Carlo simulation (Kim et al., 2011). Also, by introducing uncertainty in the demand of bioethanol and sugar, a multi-scenario mixed-integer linear programming supply chain was optimized using a sample average approximation strategy (Kostin et al., 2012). Another optimization methodology for supply chain network, which included uncertainties from the fuel market, feedstock yield and cost of logistics, employed a two-stage stochastic programming model considering conditional value at risk (Kazemzadeh, 2013).

For biorefinery optimization under technical uncertainties, a global sensitivity analysis is required for choosing the most significant parameters. For instance, a framework for model-based optimization under uncertainty, which considered four different process configurations, utilized uncertainty analysis for determining the impact of these parameters. Later, the process operation variables were optimized through Monte-Carlo simulation (Morales-Rodriguez et al, 2012). Geraili & Romagnoli (2015) developed another framework for optimizing biorefineries while

integrating the strategic and operational level. In this approach, uncertainties were considered only at the strategic level. Market prices were modeled assuming a market driven by petroleum since it happens to be the main competitor for energetics. Once the strategic level was optimized under uncertain conditions, the operation variables were optimized with a differential evolution algorithm. An extension of this work, in which uncertainty for both levels was considered, a sensitivity analysis was implemented for determining the main uncertain sources at the operational level. In this new approach, operating conditions were optimized using Monte-Carlo simulation for obtaining high profitability while considering risk management of the business (Geraili et al., 2016).

2.2 Framework design

The current optimization framework is a continuation of the previous work developed by Geraili et al. (2016). Uncertainties at the operational level are explored more carefully, and a new metaheuristic optimization mechanism is employed. The dimensionality of the problem increases as well in order to evaluate the robustness of the optimization algorithm when considering uncertainty.

In order to optimize the operating conditions of the plant under technological uncertainties four main steps are required. Identification of significant uncertain parameters through global sensitivity analysis (simultaneously and independently per product pathway), detailed simulation of processes and unit operations in the simulation software(s) under uncertainty (nonlinear model), optimization of the operating conditions of the plant by seeking the best points using the Parallel Local Metric Stochastic RBF with restart algorithm, and statistical evaluation of results previous final implementation. Figure 2 shows a general schematic structure of the proposed framework.

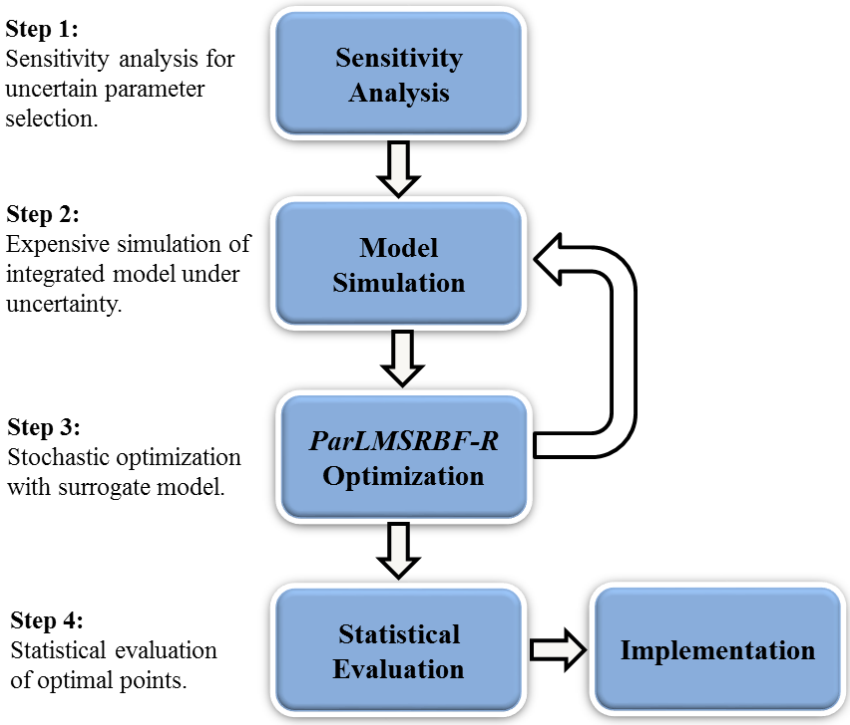

Figure 2: Framework for stochastic optimization of uncertain biorefineries

2.3 General objective function

The objective function to be maximized has F decision variables as input data, and, as explained by Geraili et al. (2014), it is the cash flow after tax of a renewable business. This function considers the total sold products, cost of raw materials, operational expenses, labor, and taxes (credits and liabilities). Since the model considers uncertainty, it runs stochastically D simulations with H different and randomly generated uncertain parameters (selected as presented in Chapter 3). However, the general objective function is composed of a group of results. It represents an *F-dimensional* problem composed of D cash flow after tax results for a certain group of F decision variables. It is assumed that the population of D results has a normal distribution and represents the general objective function. Also, this group of results denote the expensive function to be optimized by the presented framework. In order to improve the simulation resolution, Aspen Plus is linked with the numerical computing software Matlab through ActiveX Automation technology,

which permits Aspen Plus to transfer data from and to other Windows applications. Figure 3 shows a representation of the interaction between Matlab and Aspen Plus, and how the normal distribution is obtained. The distribution results are computed in Matlab.

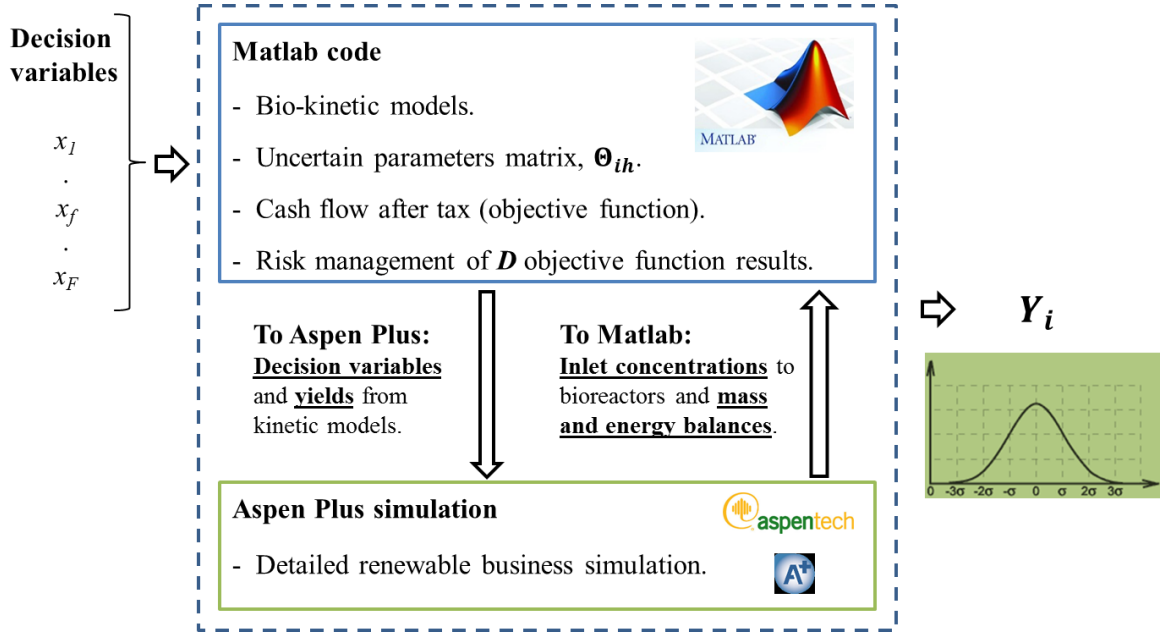

Figure 3: Matlab and Aspen Plus interaction for computing general objective function

2.4 Lignocellulosic Multi-Product Biorefinery modelling

In the following case study, the proposed framework is tested with the stochastic optimization of a hypothetical multi-product biorefinery. The lignocellulosic biorefinery is integrally modelled in the simulation software Aspen Plus guaranteeing a rigorous process simulation of the plant, able to represent complex nonlinear processes and unit operations. The biorefinery model is linked with a complex kinetic model of bio-reactions previously implemented in Matlab in which the kinetic parameters are varied for simulating uncertainty following the previous work done by Geraili et al. (2016).

The feedstock material used is lignocellulose in the form of switchgrass, and the main desired products are biofuels and value-added chemicals. Even though other feedstocks can be used for obtaining lignocellulosic material, the simulation assumes a sample feedstock whose chemical composition is similar to switchgrass. The conversion pathway used is via the sugar platform with two main products from biochemical reactions, bioethanol and succinic acid, as secondary products, heat, bioelectricity and treated water are obtained as well.

The selected scheme is composed of six major treating units. Including, raw material pretreatment, sugar hydrolysis, sugar fermentation, product purification, heat and power generation, and wastewater treatment. The optimal configuration utilized in the current work comes from a previous work (Geraili et al., 2014) that tested different process arrangements, and selected the current one as the most adequate. Figure 4 shows the actual processes implemented in the integrated multiproduct biorefinery. The independent sub-processes are:

i. Low concentration acid pretreatment for breaking the structures of the feedstock material into smaller pieces of hemicellulose, lignin and cellulose while increasing the fragmentation of cellulose;
ii. Ammonia conditioning for detoxification and pH stabilization of pre-treated biomass;
iii. Simultaneous enzymatic hydrolysis and co-fermentation for ethanol production;
iv. Separate hydrolysis and fermentation for succinic acid production;
v. Ethanol purification with distillation columns and molecular filtration;
vi. Solid separation for extracting residual solids;
vii. Succinic acid recovery using a configuration based on cell filtration followed by crystallization;

viii. Anaerobic and aerobic digestion of organic materials contained in the produced waste water from biorefining processes, and

ix. Combined system of combustion, boiler, and turbo-generator for steam and electricity production.

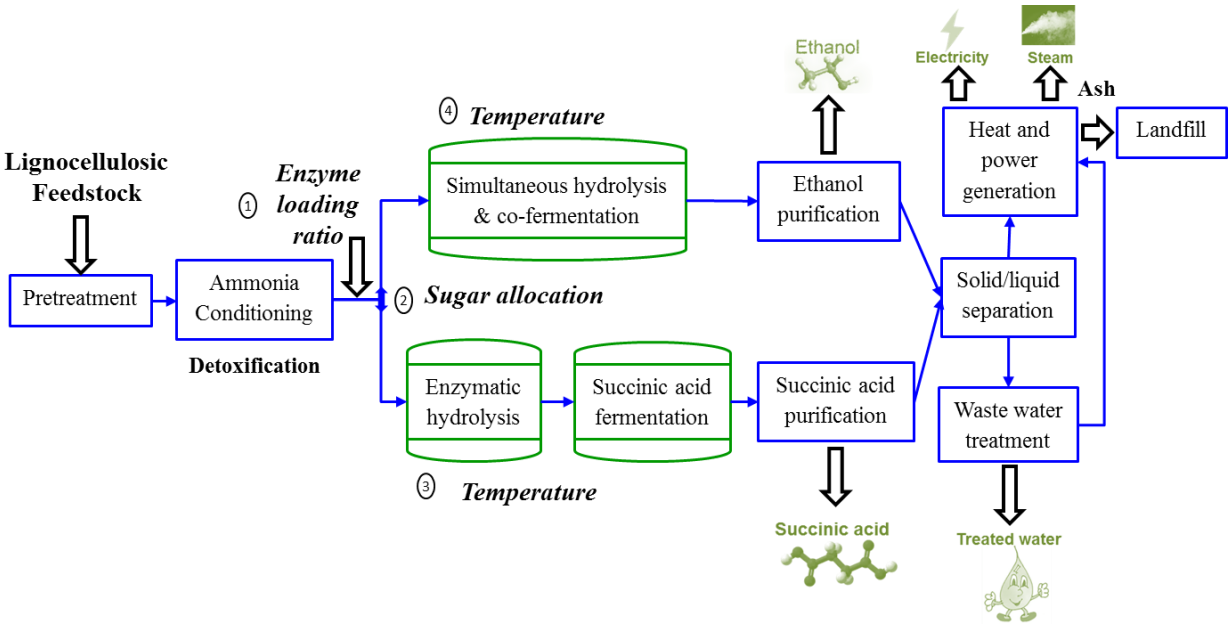

Figure 4: Multiproduct biorefinery block diagram plant and process variables to be optimized

As presented in Figure 4, the operational variables of interest that aim to be optimized are four: enzyme loading ratio, sugar allocation for bioethanol production, temperature of enzymatic hydrolysis in succinic acid production, and temperature of simultaneous enzymatic hydrolysis and co-fermentation for ethanol production. All in all, the integrated multiproduct biorefinery simulation represents a *4-dimentional* highly non-linear optimization problem. Information related to succinic acid production, including operational and economic data, was obtained from Vlysidis et al. (2011). Furthermore, operational expenditures, product yields and energy information for bioethanol production was obtained from previous works in technical and economic studies for production of cellulosic bioethanol (Humbird et al., 2011; Kazi et al., 2010). Finally, the

biochemical reactions' models implemented in Matlab for rigorous simulation of bioethanol and succinic acid production where obtained from trustworthy sources from literature (Kadam et al., 2004; Morales-Rodriguez et al., 2012; Song et al., 2008). Values and data from literature are used as starting points and reference estimates during the global sensitivity analysis and optimization.

3. SENSITIVITY ANALYSIS

3.1 Literature Review

Uncertainties can be found in different parts of a renewable energy business, from volatility in the market to the process itself. The most common uncertainties that have been studied in renewable energy endeavors come from the strategic planning stage. At operational level, uncertainties can be found in the process itself, and a global sensitivity analysis is required for choosing the most representative parameters for modelling uncertain conditions. Operational level uncertainties may be introduced to the process mainly because of errors in experimental measurements, activity changes in microorganisms involved in biochemical reactions, impurities of the chemical species, and external factors. A complete list of all the kinetic parameters and their description is provided in the Appendix. The current study aims to evaluate sensible parameters following two different approaches. The first approach is to evaluate all the parameters simultaneously. The second, to evaluate the parameters independently per product pathway.

In general, a sensitivity analysis studies the variations of the output value of a system respect to changes in its input parameters. A robust sensitivity method was developed by the Russian mathematician I. M. Sobol' (1993). Sobol's method is a variance-based Monte-Carlo technique, and in its standard form a function $Y = f(z_1, \dots, z_q, .., z_Q)$ defined as a *Q-dimensional* cube $\boldsymbol{K}^Q$ can be decomposed as presented in Ec. (1) if it is assumed that the input parameters are independent.

$$Y = f_0 + \sum_{q=1}^{Q} f_q(z_q) + \sum_{1 \le q < b \le Q} f_{qb}(z_q, z_b) + \cdots + f_{1,2,\cdots,Q}(z_1, \dots, z_Q) \tag{1}$$

The current study considers that the function Y is the objective function explained previously in Chapter 2, and the parameters $z_1, \dots, z_q, .., z_Q$ are the kinetic models' parameters listed in the Appendix. The first evaluation includes all the parameters simultaneously, and the second evaluation considers independently the parameters involved in ethanol and succinic acid production. Eq. (2) shows how the variance of Y is split.

$$V(Y) = \sum_{q=1}^{Q} V_q + \sum_{1 \le q < b \le Q} V_{qb} + \cdots + V_{1,..,q,...,Q} \tag{2}$$

The values of $V_q, V_{qb}, V_{1,\cdots,q,\cdots,Q}$ symbolize the individual variance of $f_q, f_{qb}, f_{1,\cdots,q,\cdots,Q}$ respectively. Eq. (3) shows how the parameter z_q's first-order sensitivity index is calculated.

$$\hat{S}_q = \frac{\hat{V}_q}{\hat{V}} \tag{3}$$

The first-order sensitivity index allows to rank and select from all parameters the most sensitive ones depending on the individual importance of their contribution in changing the variance of the evaluated function. Therefore, the main effect of variating the parameter z_q on the output value Y is measured. Furthermore, the total sensitivity index for the parameter z_q is calculated as Eq. 4 denotes.

$$\hat{S}_{Tq} = 1 - \frac{\hat{V}_{-q}}{\hat{V}} \tag{4}$$

The total sensitivity index evidences the sum of all the effects involving the parameter z_q since $\hat{V}_{-q}$ is the sum of all variance terms that do not include this parameter.

An improvement of the standard Sobol's method was initially presented by Homma & Saltelli (1996) and completed some years later by one of the original authors (Saltelli, 2002). The main

improvement of this method was to reduce its computational effort. However, since the current case study involves highly non-linear functions and complex bio-kinetic models, a more efficient approach is required.

The Sobol' indices to be calculated in this study follow the efficient computational method for global sensitivity analysis developed and tested by Wu et al. (2011) which is an improvement of the method developed by Homma & Saltelli (1996; Saltelli, 2002). This method reduces computational effort by averaging the results of the evaluated functions and uses those points as data which increases the size of the original sample (Wu et al, 2011).

3.2 Sensitivity indices calculation methodology

Using the previously defined single objective function, the first and total sensitivity indices are calculated for Q parameters. The algorithm is composed of the following steps:

1) Define the sample dimension *N* for the input parameters, and for each parameter define an uncertainty class. Class 1 correspond to 5% of change, and class 2 to 20% of change with respect to its default value.
2) Build two random matrices, $\boldsymbol{M_1}$ and $\boldsymbol{M_2}$, of dimensions $N \times Q$. The first matrix will be known as the 'sampling' and the second the 're-sampling' matrix.

$$\boldsymbol{M_1} = \begin{bmatrix} z_{11} \cdots & z_{1q} \cdots & z_{1Q} \\ \vdots & \vdots & \vdots \\ z_{N1} \cdots & z_{Nq} \cdots & z_{NQ} \end{bmatrix} \qquad \boldsymbol{M_2} = \begin{bmatrix} z'_{11} \cdots & z'_{1q} \cdots & z'_{1Q} \\ \vdots & \vdots & \vdots \\ z'_{N1} \cdots & z'_{Nq} \cdots & z'_{NQ} \end{bmatrix}$$

3) Generate a matrix $\boldsymbol{N_q}$ formed by all the columns of matrix $\boldsymbol{M_2}$, except the column of the z_{q} parameter, which is pulled from $\boldsymbol{M_1}$. Consecutively, generate another matrix $\boldsymbol{N_{Tq}}$ formed with all columns of $\boldsymbol{M_1}$ and with the column of the z'_q parameter, pulled from $\boldsymbol{M_2}$.

$$\boldsymbol{N_q} = \begin{bmatrix} z'_{11} \cdots & z_{1q} \cdots & z'_{1Q} \\ \vdots & \vdots & \vdots \\ z'_{N1} \cdots & z_{Nq} \cdots & z'_{NQ} \end{bmatrix} \qquad \boldsymbol{N_{Tq}} = \begin{bmatrix} z_{11} \cdots & z'_{1q} \cdots & z_{1Q} \\ \vdots & \vdots & \vdots \\ z_{N1} \cdots & z'_{Nq} \cdots & z_{NQ} \end{bmatrix}$$

4) Evaluate the row vectors with the objective function maintaining constant values for the decision variables. Each simulation runs with each sample of parameters from matrices $\boldsymbol{M_1}$, $\boldsymbol{M_2}$, $\boldsymbol{N_q}$, and $\boldsymbol{N_{Tq}}$. The values of the objective function are obtained in column vectors and are illustrated as:

$\boldsymbol{y} = f(M_1), \qquad \boldsymbol{y_R} = f(M_2), \qquad \boldsymbol{y'} = f(N_q), \qquad \boldsymbol{y'_R} = f(N_{Tq})$

5) Finally, the Sobol's indices are calculated based on scalar products of the aforementioned vectors:

$$\hat{f}_0 = \frac{1}{2N} \sum_{n=1}^{N} (\boldsymbol{y} + \boldsymbol{y_R}) \tag{5}$$

$$\gamma^2 = \frac{1}{2N} \sum_{n=1}^{N} (\boldsymbol{y} \cdot \boldsymbol{y_R} + \boldsymbol{y'} \cdot \boldsymbol{y'_R}) \tag{6}$$

$$\hat{V} = \frac{1}{2N} \sum_{n=1}^{N} (\boldsymbol{y}^2 + \boldsymbol{y_R}^2) - \hat{f}_0^{\,2} \tag{7}$$

$$\hat{V}_q = \frac{1}{2N} \sum_{n=1}^{N} (\boldsymbol{y} \cdot \boldsymbol{y_R'} + \boldsymbol{y_R} \cdot \boldsymbol{y'}) - \gamma^2 \tag{8}$$

$$\hat{V}_{-q} = \frac{1}{2N} \sum_{n=1}^{N} (\boldsymbol{y} \cdot \boldsymbol{y'} + \boldsymbol{y_R} \cdot \boldsymbol{y'_R}) - \gamma^2 \tag{9}$$

The algorithm runs three times. First, for evaluating all the parameters simultaneously, $Q_{total} = 86$. Second, for evaluating the parameters involved in bioethanol production, $Q_{bioethanol} = 49$. Third, for evaluating the parameters involved in succinic acid production, $Q_{succinic\ acid} = 37$.

3.3 Case Study 1: sensitivity indices calculated simultaneously

When all 86 parameters are evaluated simultaneously through sensitivity analysis and extensive Monte-Carlo simulations, their first and total sensitivity indices show that some parameters are relatively insensitive. The insensitive parameters are neglected and their values are considered continuous for simplify the stochastic model and reducing the complexity of the expensive function.

The first order and total sensitivity indices of the relevant sensitive parameters are presented in Figure 5 & Figure 6, respectively. In brief, 18 kinetic parameters are significantly contributing with uncertainty on the cash flow of the biorefinery. Also, the results evidence that a highest uncertainty is introduced by the parameters involved in enzymatic hydrolysis and fermentation of sugars for succinic acid production.

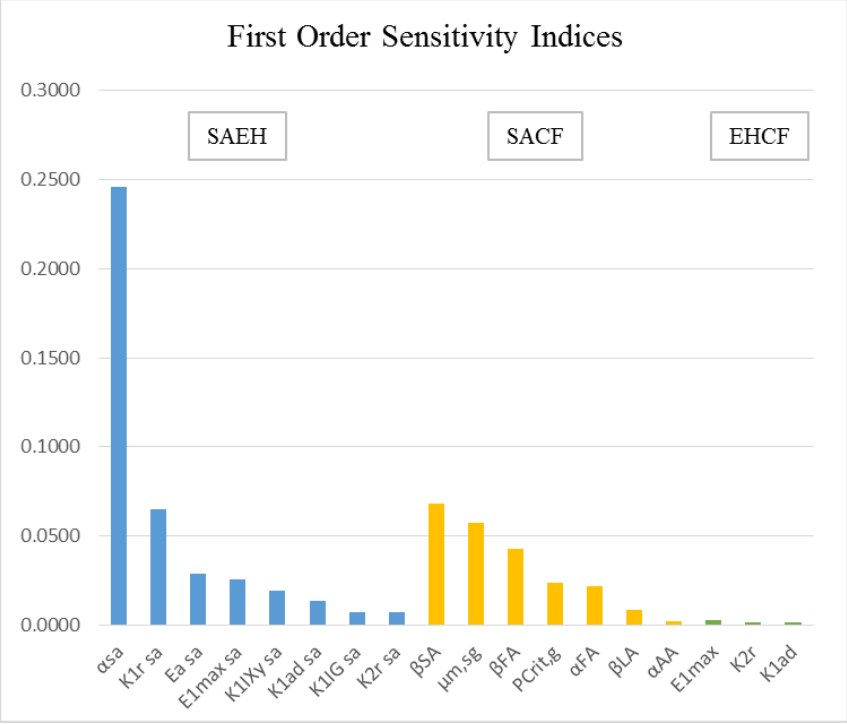

Figure 5: First order sensitivity indices of cash flow calculated simultaneously

This result is expected when all the parameters are evaluated simultaneously. Succinic acid has a higher price than ethanol in the market, and a higher cost of separation. Consequently, the sensitivity analysis is alerting that when considering operational level uncertainty, succinic acid production will have a leading role in the multiproduct biorefinery optimization problem because its bio-kinetic model's parameters introduce higher uncertainty. On the other hand, the sensitivity analysis shows low sensitivity in the parameters from simultaneous hydrolysis and co-fermentation of bioethanol. For optimizing the biorefinery (Chapter 4) $H = 18$ is considered for this case scenario.

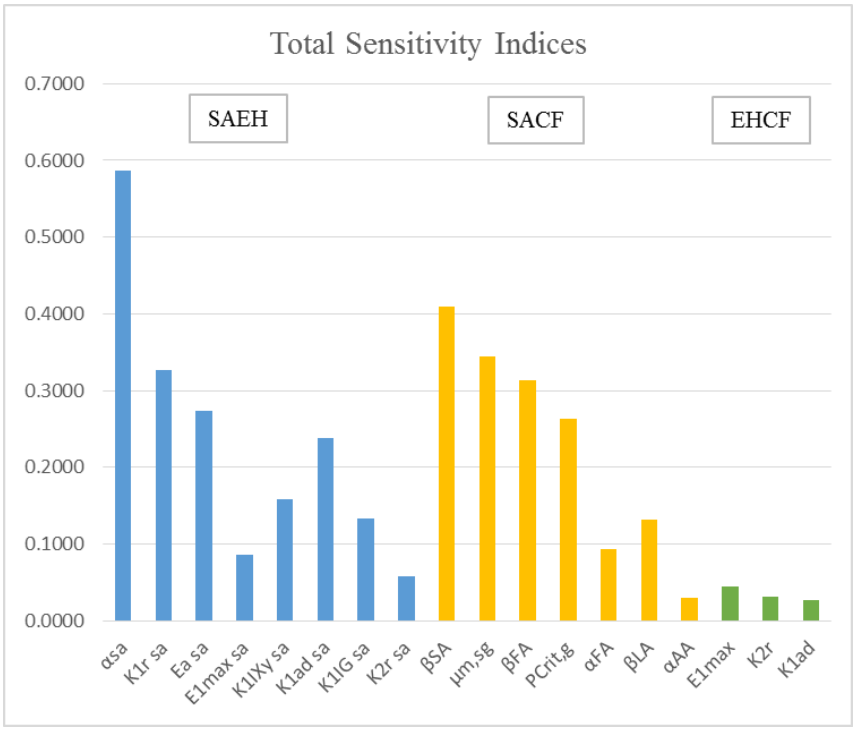

Figure 6: Total sensitivity indices of cash flow calculated simultaneously

Figure 5 & Figure 6 show that in the enzymatic hydrolysis of sugars for succinic acid production, the conversion rate of cellulose to cellobiose is an important step in the reaction mechanism and a possible rate limitting step in the reaction pathway. Also, high sensitivity in α_{sa}, $K_{1r\,sa}$, $E_{a\,sa}$ and $E_{1\,max\,sa}$ insinuate that the competition in glucose consumption between formic acid

and succinic acid production is significant and determinant in the profitability of the analyzed renewable energy business. Thus, adequate operational conditions will minimize the risk of glucose conversion to formic acid and increases succinic acid production. In other words, increase the profitability of the biorefinery due to the minimization of undesired products. Since ethanol has a lower value in the market, three parameters appear to be significant sources of uncertainty. During simultaneous hydrolysis and co-fermentation for ethanol production only the enzymatic hydrolysis stage contributes with uncertainty.

3.4 Case Study 2: sensitivity indices calculated per product pathway

Evaluating the kinetic parameters independently for each product aims to treat each process as an autonomous section of the biorefinery whose uncertainty requires to be considered individually. In the following evaluation, the sensitivity analysis is done first for the 49 kinetic parameters related to bioethanol production and later for the next 37 parameters present in the kinetic model of succinic acid production. As in the previous evaluation, the obtained first and total sensitivity indices show that some parameters are relatively insensitive. However, since the evaluation is run independently, bioethanol's kinetic parameters have a higher contribution than before.

After extensive Monte-Carlo simulations and mathematical operations it is found that from 49 parameters present in bioethanol production, 8 parameters arise to be sensitive. Similarly, from 37 parameters that conform the kinetic model of succinic acid production, 10 parameters appear to be sensitive. This result shows a more distributed uncertainty which intends to avoid the bias from evaluating all the parameters simultaneously and will accurately adjust to changes in the objective function. For optimizing the biorefinery (Chapter 4) an $H = 8 + 10$, or $H = 18$ is considered for this case scenario. Figure 7 & Figure 8 present the first order and total sensitivity indices for

bioethanol, and Figure 9 & Figure 10 show the first order and total sensitivity indices for succinic acid production.

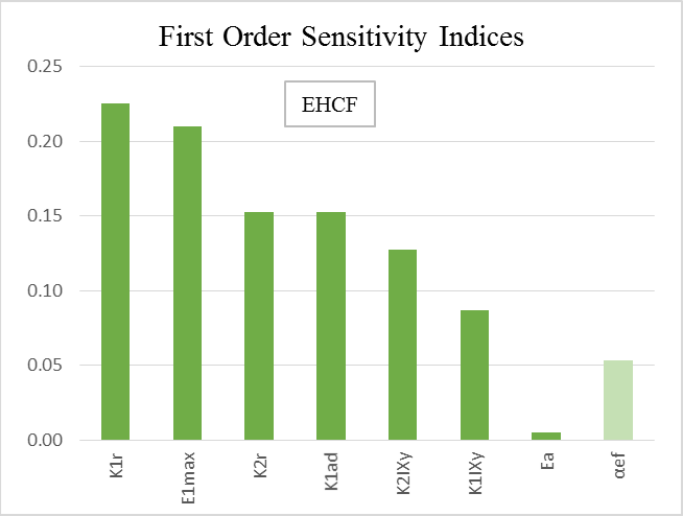

Figure 7: First order sensitivity indices of cash flow calculated for bioethanol acid production

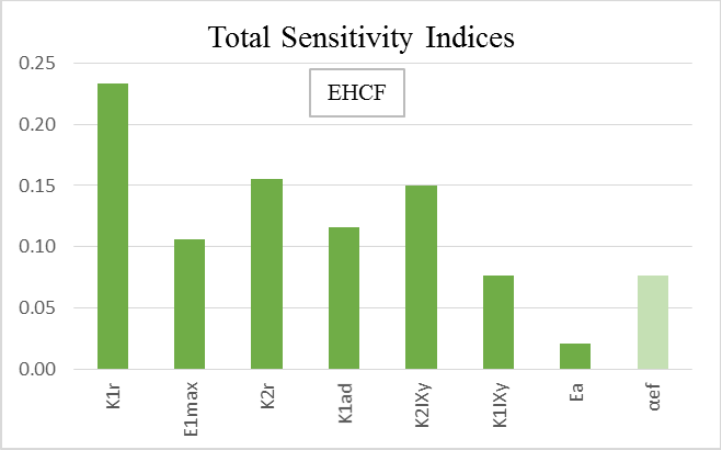

Figure 8: Total sensitivity indices of cash flow calculated for bioethanol production

From Figure 7 & Figure 8, results indicate that in simultaneous saccharification and co-fermentation for ethanol production, the hydrolisis stage presents more sensitive parameters (7 out of 8). The sobol indices of parameters K_{1r}, $E_{1\,max}$, K_{1IXy} and K_{1ad}, who have a positive effect in the production of cellobiose from cellulose suggest that this reaction is important in the production of

ethanol since their indices' value is high. The cellulose to cellobiose reaction can be considered as a bottle neck in the reaction pathway. On the other hand, only one factor was identified sensitive in the co-fermentation stage. α_{ef}, the weighing factor for glucose consumption, shows that for the cell growth, the consumption of glucose is a key factor in ethanol production.

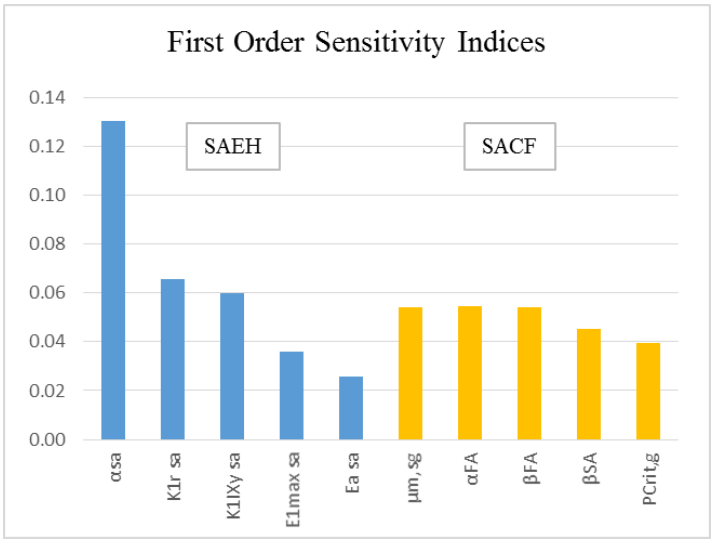

Figure 9: First order sensitivity indices of cash flow calculated for succinic acid production

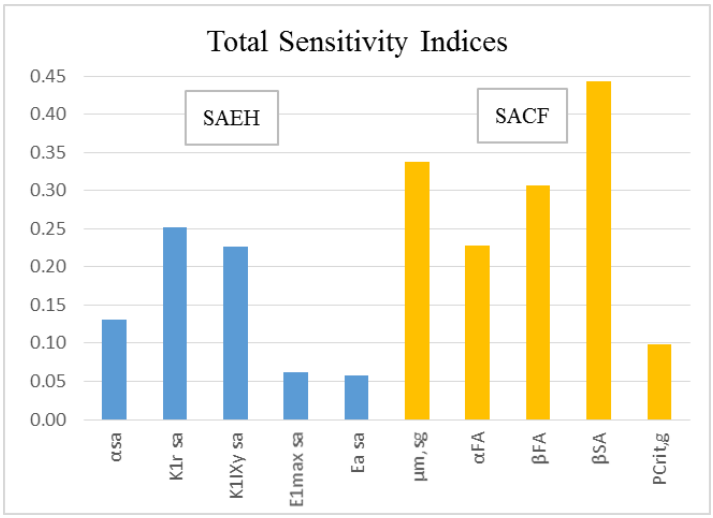

Figure 10: Total sensitivity indices of cash flow calculated for succinic acid production

Figure 9 & Figure 10 are consistent with the sensitive parameters obtained when all the parameters are evaluated simultaneously. The parameters α_{sa}, $K_{1r\ sa}$, $K_{1IXy\ sa}$, $E_{1\ max\ sa}$ and $E_{a\ sa}$, similarly like in hydrolysis for ethanol production, point out the importance in cellobiose generation. The conversion of cellulose to cellobiose has again an important role in the reaction mechanism. In succinic acid fermentation, $\mu_{m,sg}$, α_{FA}, β_{FA}, and β_{SA}, show high sensitivity. These parameters show that succinic acid production and formic acid production compete between each other in glucose consumption. Therefore, the proper conditions will reduce formic acid, and increase succinic acid which translates in higher profitability of the biorefinery.

4. STOCHASTIC RBF ALGORITHM FOR GLOBAL OPTIMIZATION

4.1 Literature Review

Global optimization problems of expensive functions hold the features of non-linearity, non-convexity and possess substantial local optima solutions. Engineering is a field where surrogate models have helped to achieve optimization requirements, particularly in *n-dimensional* problems that involve complex simulations. The optimization strategies that take advantage of surrogate models can be classified in three main groups. The first strategy, traditional sequential approach, requires a quite large number of sample points. The surrogate model is optimized once fitted. The second approach uses a validation or optimization loop which decides resampling or remodeling if defined criterion are not met or accuracy improvement is needed. The third strategy obtains the optimal point by generating guided adaptive sampling points (Wang & Shan, 2007). A previous work in global optimization of complex bioprocesses took advantage of surrogate models for different dynamic optimization problems in which optimal operating conditions were searched. After comparing the results with other metaheuristic approaches, the author concludes that surrogate model-based optimization requires less function evaluations (Egea, 2008).

As a form of surrogate or meta-model, radial basis functions (RBF) have a wide variety of applications in optimization problems. Its multivariable approximation provides valuable properties. Literature indicates that different types of RBF can converge when seeking the global optima of expensive functions without requiring vast assumptions, and it concludes that this method is similar to a statistical global optimization approach (Gutmann, 2001). Furthermore, a RBF expansion has been employed for approximating the numerical solution of weakly singular Volterra integral equations, demonstrating its capability to simplify complex functions (Galperin & Kansa, 2002). A more elaborated global optimization methodology using RBF was developed

by Regis & Shoemaker (2007a, 2009). The metric stochastic response surface framework studied the calibration of ground water bioremediation parameters by minimizing the total squared residual error. Even though several studies have addressed global optimization using surrogate modelling, none of them have optimized operational variables while simulating uncertainty. The present work implements a stochastic RBF algorithm for optimizing a multiproduct biorefinery modelled under two different approaches of uncertainty at operational level.

4.2 Optimization objective function considering uncertainty

When sources of uncertainty are introduced to the renewable energy business model, the individual objective function, as presented in Figure 4, can be written in the form of Equation 10. The individual objective function is evaluated stochastically D times the population of uncertain parameters is generated.

$$Y_i = c^T x + E_s[f(x, \Theta_{ih})] \tag{10}$$

Constraints:

$$w(x) = 0 \tag{11}$$

$$z(x) \leq d_l \tag{12}$$

$$\Theta_i^{LB} \leq \Theta_i \leq \Theta_i^{UB} \tag{13}$$

The objective function that considers uncertainty, has a deterministic term $c^T x$, where c^T represents a constant vector and x the decision variable vector. Uncertainties are deemed in the term $E_s[f(x, \theta_h)]$ which is the expected value representing uncertainty as a function of the decision variables, x, and uncertain parameters, Θ_h. For limiting the individual objective function, the vectors $w(x)$ and $z(x)$ are the set of equality and inequality constraints, respectively.

The uncertain parameters matrix, Θ_{ih}, is generated using a sampling technique, e.g. Latin Hypercube Sampling. The dimension of the matrix is $D \times H$, where D is the number of individual simulations required to obtain a representative uncertain population and H is the total number of uncertain parameters.

$$\boldsymbol{\Theta_{ih}} = \begin{bmatrix} \theta_{11} \cdots & \theta_{1h} \cdots & \theta_{1H} \\ \vdots & \vdots & \vdots \\ \theta_{i1} \cdots & \theta_{ih} \cdots & \theta_{iH} \\ \vdots & \vdots & \vdots \\ \theta_{D1} \cdots & \theta_{Dh} \cdots & \theta_{DH} \end{bmatrix}$$

Figure 11 shows how the optimization criteria is defined. Once the D simulations run, a normal distribution of the results is expected for a single set of decision variables. In this distribution, the population's standard deviation, σ_i, and the 2.5th percentile are calculated. The expensive function, including uncertainty, to be maximized is the 2.5th percentile of the normal distribution generated. The best set of decision variables will be the ones that obtain the highest cash flow after tax value. By stablishing the aforementioned statistical selection of decision variables, technological risk minimization is accounted in the optimization problem since the lower bound of the results is maximized.

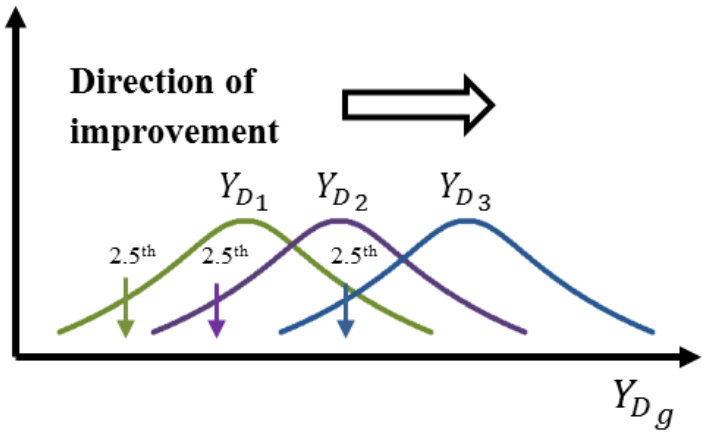

Figure 11: Risk management definition for the optimization problem

Taking advantage of the optimization methodology developed by Regis & Shoemaker (2007a; 2009) a parallel stochastic RBF algorithm is utilized. The expensive function in which the global minima will be searched, is written in the following form:

$$max\ f(x), \qquad \text{subject to } \boldsymbol{x_g^l} \leq \boldsymbol{x_g} \leq \boldsymbol{x_g^u} \tag{14}$$

Where, $\boldsymbol{x_g^l}$ and $\boldsymbol{x_g^u}$ are vectors that contain the lower and upper bound values of the decision variables of an expensive *n-dimensional* function. The interest is to maximize the 2.5th percentile. The expensive stochastic objective function is written in Equation 15.

$$f(x) = \frac{\sum_{i=1}^{D} Y_i}{D} - z_c \cdot \sigma_i \tag{15}$$

4.3 Radial Basis Function

The present study takes advantage of a RBF interpolation as the response surface or surrogate model. The RBF's parameters are updated continuously in each iteration with a point or group of points evaluated in the expensive function. From Powell's work (1992), the model fitting starts with J different input points, $x_1, x_2, \dots, x_j, \dots, x_J,\ x\ \epsilon\ \mathbb{R}^d$, where their function values are known, $f(x_1), \dots, f(x_j), \dots, f(x_J)$. The interpolation can be written in the general form presented in Equation 16.

$$s(x) = \sum_{j=1}^{J} \lambda_j \gamma\left(\|x - x_j\|\right) + p(x)\,, \mathbb{R}^d \tag{16}$$

Where, $\|\cdot\|$ is the Euclidean norm, $\lambda_j\ \epsilon\ \mathbb{R}$ for $j = 1, \dots, \mathrm{J}$. The current algorithm employs a linear polynomial tail, $p(x)$, and has a cubic form, $\gamma(r) = r^3$. Other forms of $\gamma(r)$ such as, linear, thin plate spline, Gaussian, inverse multi-quadric and multi-quadric are available as well (Powell,

1992). Later, a matrix $\Gamma \epsilon \mathbb{R}^{J \times J}$ by: $\Gamma_{jk} := \gamma\left(\left\|x_j - x_k\right\|\right)$, $\mathrm{j,k} = 1, \ldots, \mathrm{J}$ is denoted. Simultaneously, a matrix $\mathrm{P} \epsilon \mathbb{R}^{J \times (d+1)}$ is defined, and its j^{th} row is represented as $[1, x_j^T]$. Equation 17 presents the system that needs to be solved for obtaining the fitted cubic RBF.

$$\begin{pmatrix} \Gamma & P \\ P^T & 0 \end{pmatrix} \begin{pmatrix} \lambda \\ c \end{pmatrix} = \begin{pmatrix} F \\ 0_{(d+1)} \end{pmatrix} \tag{17}$$

Where, $F = (f(x_1), \ldots, f(x_J))^T, \lambda = \left(\lambda_1, \ldots, \lambda_J\right), \epsilon, \mathbb{R}^J,$ and $, \mathrm{c} = (\mathrm{c}_1, \ldots, \mathrm{c}_{d+1}) \epsilon \mathbb{R}^{d+1}$ represents the coefficients of the linear polynomial tail, $p(x)$. Notice that the coefficient matrix is invertible only if $, rank(P) = d + 1$ (Powell, 1992; Regis & Shoemaker, 2007a). Therefore, the condition $n \geq d + 1$ is mandatory.

4.4 Global Optimization Algorithm *ParLMSRBF-R*

For optimizing the expensive stochastic objective function, a parallel metric stochastic RBF algorithm is employed. The special case of the algorithm is the Parallel Local Metric Stochastic Radial Basis Function with Restart (*ParLMSRBF-R*) (Regis & Shoemaker, 2007a; Regis & Shoemaker, 2009). The algorithm seeks for the global maxima by guiding the search of optimal points in the expensive function until stop criteria is met, a complete exploration in the solution domain is guaranteed since the algorithm starts from scratch whenever it infers it has reached local optima. Likewise, it takes advantage of parallel computing evaluations, so multiple points are generated for simultaneous evaluations.

The algorithm runs following a Master-Worker criteria for parallelization. It is assumed that *P* processors are available and that two function evaluations take the same amount of time. The expensive function is evaluated with a set of initial points generated from a space-filling experimental design. With the initial results of the expensive function evaluations, the response

surface model, e.g. RBF, is fitted in each iteration. The obtained model is evaluated in P different points, which are obtained from a group of *candidate points*, utilizing P procesors. Thus, there will be running P worker plus the master task ($P + 1$). For starting the algorithm, the expensive stochastic objective function is defined as a closed hypercube $\mathfrak{D} = [a, b] \subseteq \mathbb{R}^d$; a number of processors, P, is defined; a particular response surface model, e.g., RBF, is designed as the surrogate; an initial set of evaluation points, $\mathcal{J} = \{x_1, x_2, \dots, x_{n_o}\}$, is generated based on a space-filling experimental design ($n_o = k \cdot P$ and k is a positive integer); the number of candidate points per iteration, t, is set ($t \gg P$), and a maximum number of expensive function evaluations, N_{max}. When N_{max} expensive function simulations are completed ($n = N_{max}$), the algorithm stops. From the set of n previously evaluated points, $\mathcal{A}_n = \{x_1, x_2, \dots, x_n\}$, the outputs are points at which the stochastic objective function is minimized. It also represent the optimal operating conditions for the biorefinery (Regis & Shoemaker, 2009). The *ParLMSRBF-R*'s steps are described as follows:

i. Initialize the master and the P worker tasks while an initial experiment $\mathcal{J}$ is generated.
ii. The master distributes uniformly the initial points generated in (i) to the P workers. Each worker evaluates the expensive simulation model at the given points, the results return to the master which waits until all workers are done with their tasks. For each result, the master updates the best value found.
iii. The master initializes the algorithm parameters (Table 1 shows the parameter values employed in this work), and $n = k \cdot P$, $\mathcal{A}_n = \mathcal{J}$ are set. While the termination criteria has not being met, the algorithm proceeds as described,
    a. The master fits or updates the surrogate model $s_n(x)$, e.g., RBF, using the data points generated in (i) and (ii), referred as $\mathcal{B}_n = \{(x, f(x)) : x \in \mathcal{A}_n\} = \{(x_i, f(x_i)) : i = 1, \dots, n\}$.

b. A set of t random *candidate points*, $\Omega_n = \{w_{n,1}, \dots, w_{n,t}\}$, is generated following a probability distribution, e.g., random perturbations, in $\mathbb{R}^d$. These points are normally distributed with zero mean and covariance matrix $\sigma_n^2 I_d$, where $\sigma_n = \rho_n \ell(\mathfrak{D})$. The length of one side of the hypercube is denoted as $\ell(\mathfrak{D})$ where the condition $\inf_{n \geq n_o} \rho_n > 0$ is mandatory; σ_n is defined as the *step size*.

c. The master selects a set $\mathfrak{F}_n = \{x_{n+1}, \dots, x_{n+P}\}$ of P evaluation points from the t *candidate points* generated in Ω_n using the information from the fitted and/or updated response surface model $s_n(x)$ and the $\mathcal{B}_n$ data points. The master distributes evenly to the P workers, the P selected evaluation points.

d. Every worker evaluates the expensive simulation model at the given points and the results are sent back to the master task.

e. For all the results returned by each worker, the master waits until all workers finish their tasks and updates the best function value obtained. Finally, the master updates the algorithm parameters, including the probability distribution ones. $\mathcal{A}_{n+P} := \mathcal{A}_n \cup \mathfrak{F}_n$ is set and $n := n + P$ reset.

End.

iv. The best solution found, $x_{N_{max}}{}^*$, is returned.

The algorithm achieves exploitation by keeping track of the consecutive failed and successful synchronous parallel iterations, denoted by C_{fail} and $C_{success}$ respectively. Whenever C_{fail} or $C_{success}$ exceed a predefined tolerance value, $\mathcal{T}_{fail}$ or $\mathcal{T}_{success}$, the *step size* σ_n, from (b) of (iii), reduces by half or doubles respectively. The recorded values of C_{fail} and $C_{success}$ are reset to zero, and the algorithm keeps running. When the algorithm exceeds a maximum imposed limit of failed

synchronous parallel iterations $\mathfrak{M}_{fail}$, different from C_{fail}, the algorithm evidences local minima, and the entire algorithm restarts from scratch. In other words, it restarts from (i) in order to prevent the bias from the previous evaluated points employed for fitting $s_n(x)$ (Regis & Shoemaker, 2009).

Table 1: Parameter values for *ParLMSRBF-R* for global optimization

Parameter	Value
Ω_n, number of candidate points for each parallel iteration.	$500\ d$
Υ, weight pattern.	$\langle 0.3, 0.5, 0.8, 0.95 \rangle$
κ, number of weights in Υ.	4
σ_n, initial step size.	$0.2\ \ell(\mathfrak{D})$
σ_{min}, minimum step size.	$(0.1)\left(\frac{1}{2}\right)^6 \ell(\mathfrak{D})$
δ_{tol}, radius tolerance.	$0.001\ell(\mathfrak{D})$
$\mathcal{T}_{success}$, threshold parameter for deciding when to increase the step size.	3
$\mathcal{T}_{fail}$, tolerance parameter for deciding when to reduce the step size.	$\max\left(\left[\frac{d}{P}\right], \left[\frac{\lvert\kappa\rvert}{P}\right]\right)$
$\mathfrak{M}_{fail}$, maximum failure tolerance parameter.	$5\ \mathcal{T}_{fail}$

Moreover, the algorithm explores close to the best solution neighborhood in *n-dimensions*. The function evaluation point selection is done following two scored criteria. The estimated value generated by the response surface model (*response surface criterion*), and the minimum distance from previously evaluated points (*distance criterion*). The two criteria might conflict; therefore, it is required to implement a weighted score. Each candidate point is given a score between 0 and 1 in both criteria, from which a more desirable point is the one whose score is closer to 0. The standard of a good candidate point intents to have a low estimated function value and be far away from the previously evaluated point (Regis & Shoemaker, 2007a). The detailed steps implemented in (c) of (iii) can be found in (Regis & Shoemaker, 2009).

In summary, by approximating an expensive simulation model, this stochastic optimization strategy permits to reduce computational effort with a guided search in the decision variables domain while performing evaluations in parallel. Figure 12 presents a scheme of the *ParLMSRBF-R* global optimization strategy.

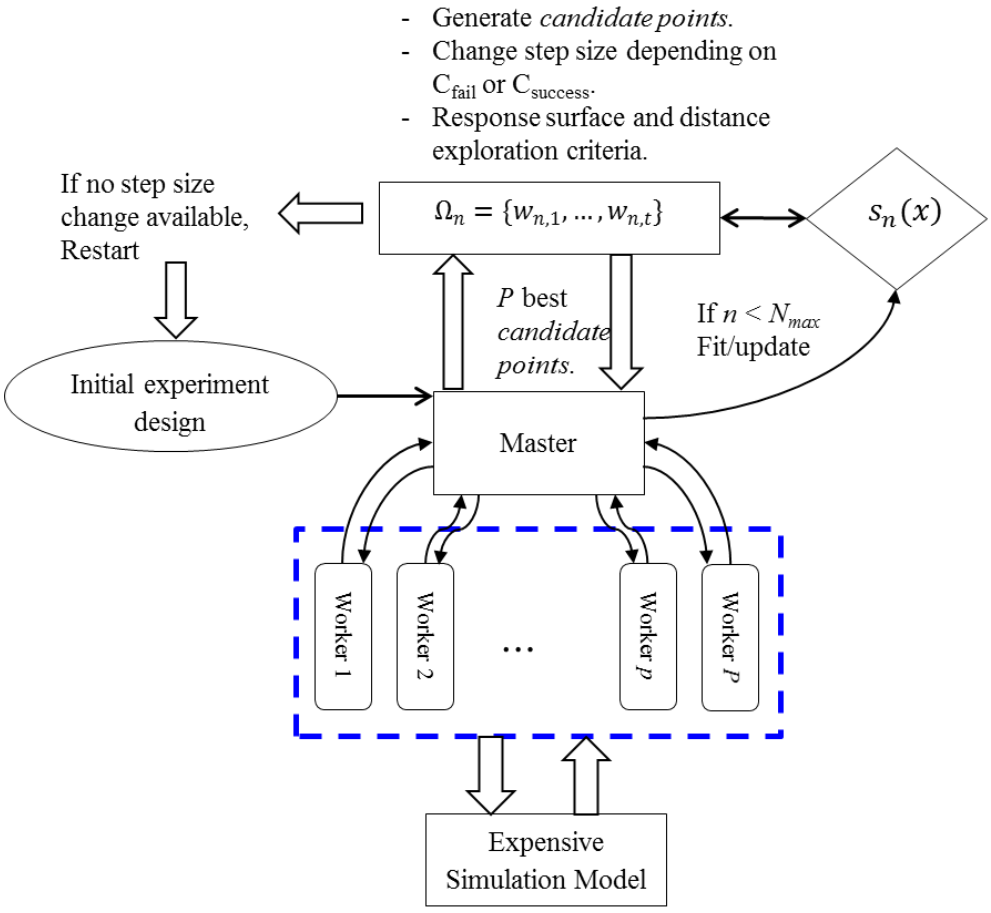

Figure 12: *ParLMSRBF-R* global optimization strategy

5. RESULTS FOR GLOBAL OPTIMIZATION

5.1 Case Study 1: *ParLMSRBF-R* method (uncertainty simultaneously calculated)

For maximizing the expensive objective function previously defined (2.5^{th} percentile of $D = 100$ stochastic simulations) under uncertainty simultaneously calculated, a Parallel Local Metric Stochastic Radial Basis Function with Restart (*ParLMSRBF-R*) algorithm is employed. The code is available in Matlab share and was developed by Regis & Shoemaker (2007a, 2009). The previous mentioned method applies a stochastic strategy that searches in the solution dominium guided better solutions with the help of a fitted and continuously updating RBF. The optimization method runs three times with different number of P new samples, the input values for each maximization evaluation are shown in Table 2.

Table 2: Evaluations with uncertainty simultaneously calculated and *ParLMSRBF-R*

Scenario	Inputs		
	N_{max}	Ntrials	New Samples, P
Evaluation 1	80	1	1
Evaluation 2	80	1	2
Evaluation 3	80	1	4

The maximum number of expensive function evaluations, N_{max}, set is 80 and only one trial. The results obtained for each run are presented in Figure 13, Figure 14 and Figure 15.

The first evaluation, presented in Figure 13, shows convergence at the 46 expensive function simulation. In this case, the algorithm restarts after the 56 expensive simulations, once σ_n cannot reduce more and local optima is identified.

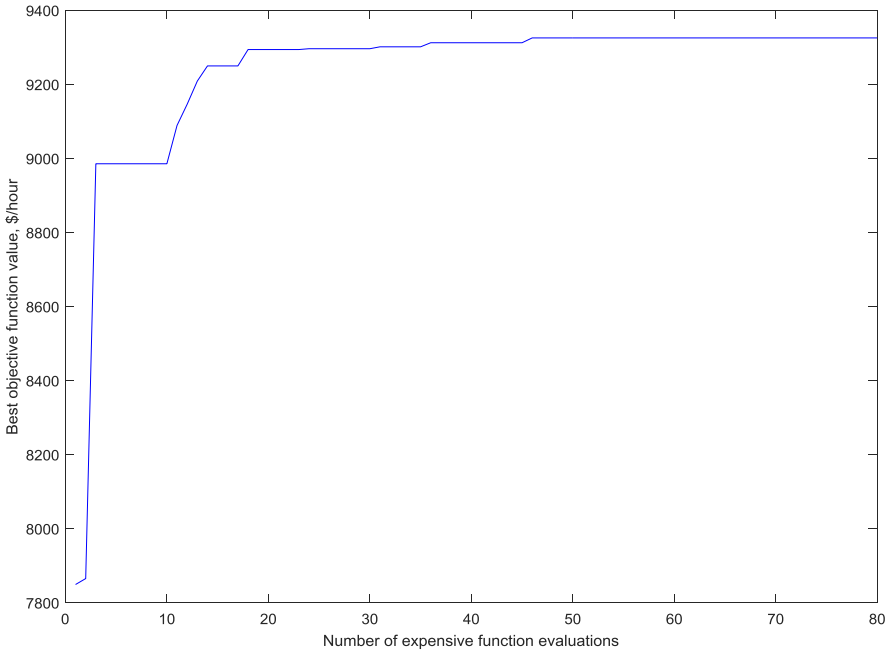

Figure 13: Convergence profile first evaluation, *ParLMSRBF-R* with uncertainty simultaneously calculated

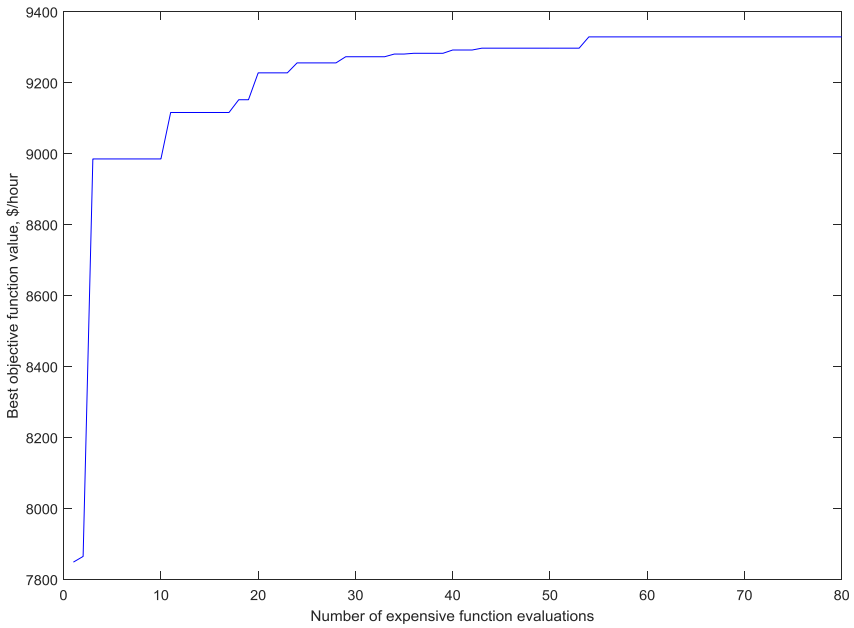

Figure 14: Convergence profile second evaluation, *ParLMSRBF-R* with uncertainty simultaneously calculated

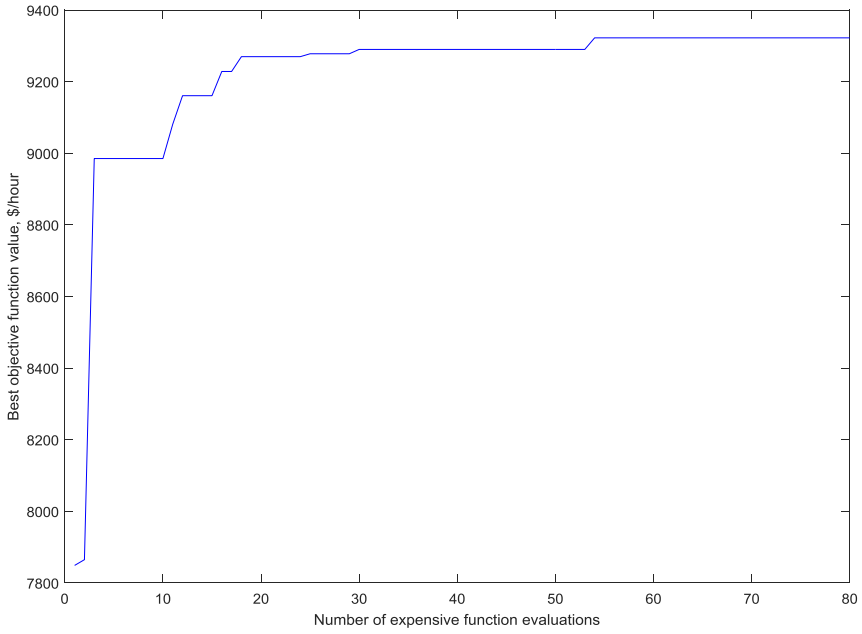

Figure 15: Convergence profile third evaluation, *ParLMSRBF-R* with uncertainty simultaneously calculated

The second and third evaluation, Figure 14 and Figure 15, respectively, show convergence at the 54 expensive function simulation in both cases. For both evaluations, the algorithm does not restart, and parallel computing or the generation of multiple points per iteration is employed with $P = 2$ and $P = 4$, respectively. The third evaluation obtains the best operating conditions that will provide the highest profitability with uncertainty simultaneously calculated while minimizing technological risk.

5.2 Case Study 1: Comparative analysis with Monte-Carlo (uncertainty simultaneously calculated)

In order to evaluate the efficacy of the global optimization method used, the obtained optima points are compared with results from Monte-Carlo simulation (MC) where 80 randomly generated points are tested following the procedure presented by Geraili et al. (2016). The two points that

provide the best output value are selected and compared with the points obtained with *ParLMSRBF-R*. Table 3 presents the best operational points.

Table 3: Best operating points (uncertainty simultaneously calculated): *ParLMSRBF-R* and Monte-Carlo simulation

	Best operating points			
Scenario	T, hydrolisis for succinic acid, [°C]	Enzyme loading ratio [g enzime/ kg cellulose]	Sugar allocation (sugar to ethanol)	T, hydrolisis and cofermentation for ethanol, [°C]
Evaluation 1	30.66	16.41	0.200	51.57
Evaluation 2	34.30	15.47	0.200	50.96
Evaluation 3	37.68	14.36	0.200	52.12
MC (38)	30.77	14.62	0.223	46.35
MC (59)	35.12	19.85	0.201	48.07

All five points, three from *ParLMSRBF-R* and two from MC simulation, are tested under same uncertain conditions ($D = 100$). From Table 4, and recalling the established criteria from Figure 11 (direction of improvement and risk management) it is determined that the best points for the hypothetical multi-product lignocellulose biorefinery are the operating conditions obtained in the third evaluation.

Table 4: Biorefinery cash flow, $D = 100$ (uncertainty simultaneously calculated)

Scenario	Cash flow, USD/h		
	2.5^{th}	Mean	97.5^{th}
Evaluation 1	9283.62	9704.00	10124.38
Evaluation 2	9291.05	9712.7	10134.36
Evaluation 3	9291.61	9717.99	10144.36
MC (38)	9130.89	9577.84	10024.79
MC (59)	9161.81	9634.38	10106.96

However, when analyzing the points, their output results yield closely. Figure 16 & Figure 17 show a Kruskal-Wallis test of significance in which the best scenario is contrasted with the other

ones. MC (38) results are significantly different from the best result. Moreover, the optimal temperatures in hydrolysis for succinic acid production, when contrasted with enzyme loading ratio, show that in optima less temperature is required when there is higher enzyme loading ratio. Also, the optimal points when using *ParLMSRBF-R* for temperature in simultaneous hydrolysis and co-fermentation for bioethanol production agree that the temperature has to increase from its original point (48 °C) when uncertainty is introduced.

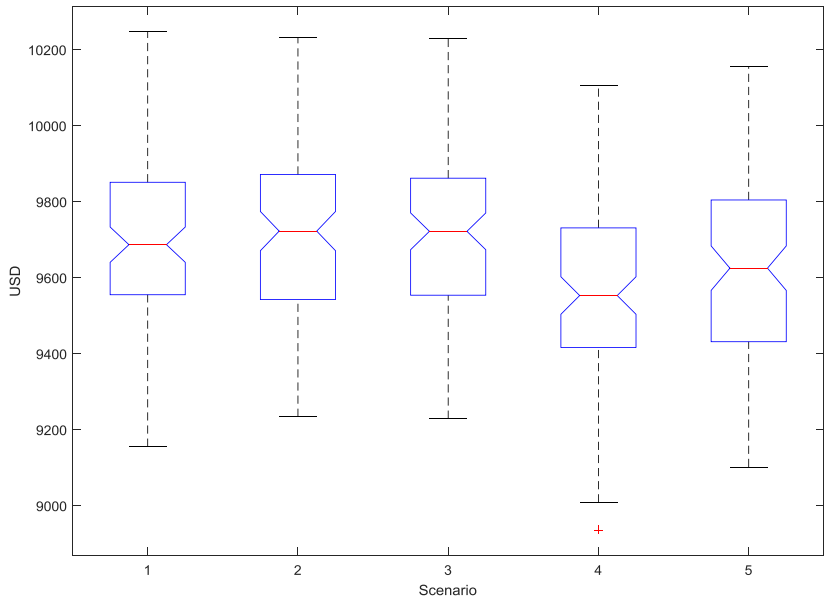

Figure 16: Kruskal-Wallis analysis for the best scenarios

Finally, Table 5 presents the improvement attained when using the points obtained with the *ParLMSRBF-R* method in contrast to the best point obtained from MC simulation. The results show that the implemented framework can improve in 1.76% the profitability of a renewable energy business in contrast to conventional methods, such as MC, while reducing the quantity of expensive simulation required for optima convergence. The *ParLMSRBF-R* method is highly competitive in terms of convergence since it obtains the optima result with less than three quarters

of expensive simulations than MC simulation. Figure 18 shows a comparison between the best result obtained (Evaluation 3) with the MC simulation's evaluated points. The three continuous lines represent the 2.5th, mean value and 97.5th percentile of the best scenario. This configuration considers technological risk minimization because the worst scenario is maximized, and as a consequence the mean and 97.5th percentile are pushed to better values. The normal distribution considers 95% of probability or 5% of significance.

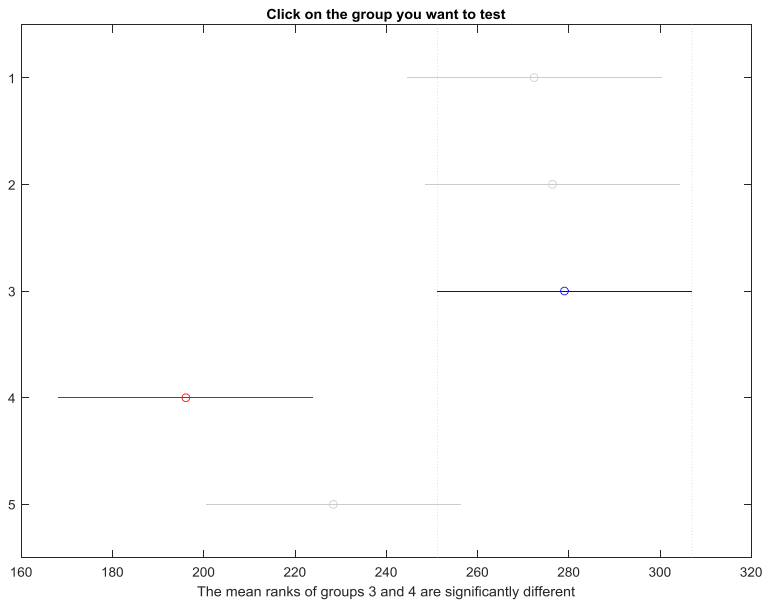

Figure 17: Statistical difference analysis for the best scenario (Scenario 3)

Table 5: Scenarios results and improvement with respect the best Monte-Carlo points

Scenario	Cash flow, USD			Improvement			Convergence
	2.5th	Mean	97.5th	2.5th	Mean	97.5th	
Evaluation 1	9283.6	9704.0	10124.4	1.67%	1.38%	1.09%	Sim. 46
Evaluation 2	9291.1	9712.7	10134.4	1.75%	1.48%	1.20%	Sim. 54
Evaluation 3	9291.6	9718.0	10144.4	1.76%	1.53%	1.31%	Sim. 54
MC (38)	9130.9	9577.8	10024.8	-	-	-	after 80 sim.

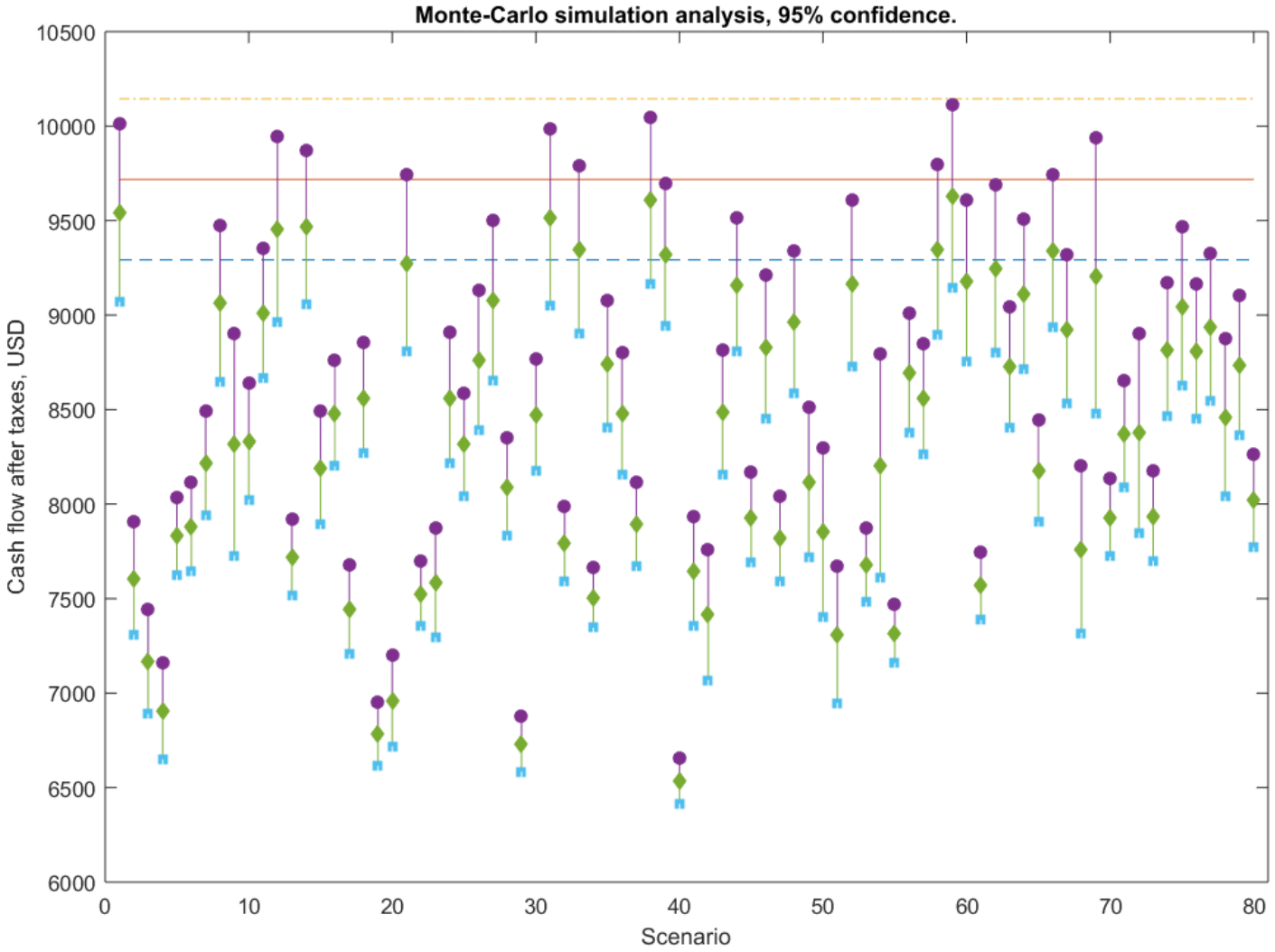

Figure 18: Comparative analysis between *ParLMSRBF-R* best scenario and Monte-Carlo method considering uncertainty simultaneously calculated

5.3 Case Study 2: *ParLMSRBF-R* method (uncertainty calculated per product pathway)

As implemented previously, for maximizing the expensive objective function under uncertainty calculated per product pathway (2.5th percentile of $D = 100$ stochastic simulations), a Parallel Local Metric Stochastic Radial Basis Function with Restart (*ParLMSRBF-R*) algorithm is employed. Similarly, the optimization method runs three times with different number of P new samples. The input values for each maximization evaluation are the same as presented in Table 2. The maximum number of expensive function evaluations, N_{max}, is 80 and only one trial. The results obtained for each evaluation are presented in Figure 19, Figure 20 and Figure 21.

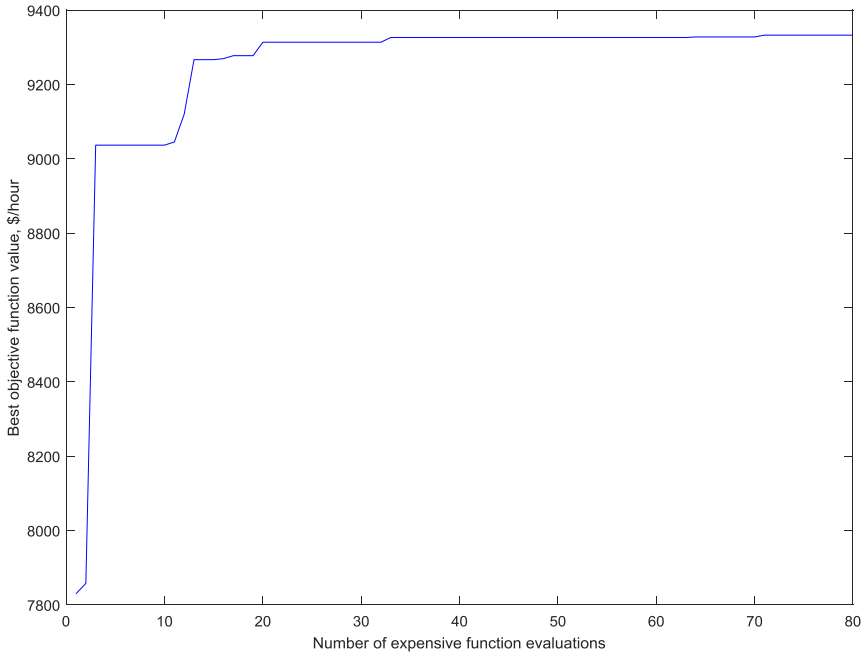

Figure 19: Convergence profile first evaluation, *ParLMSRBF-R* with uncertainty per product pathway

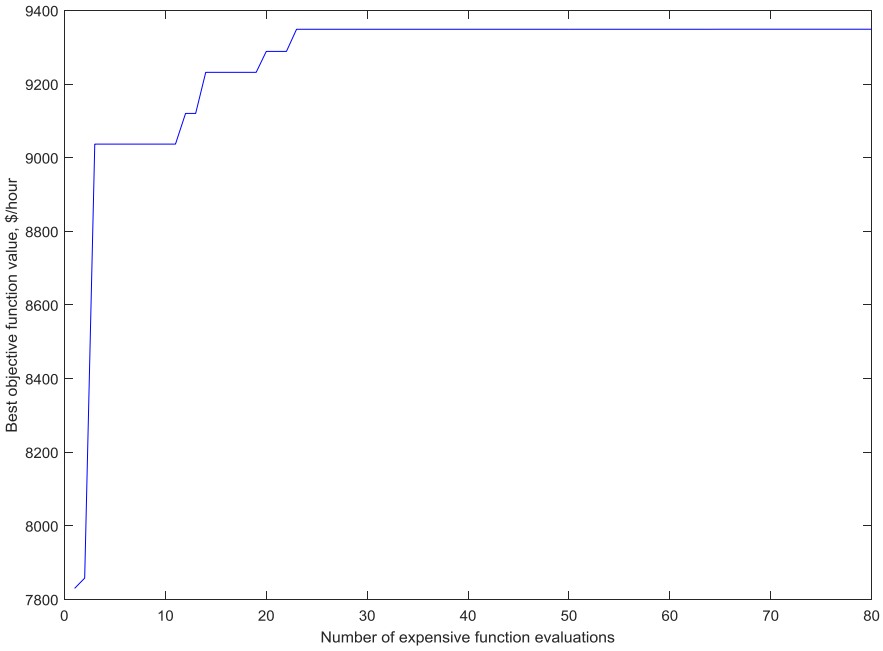

Figure 20: Convergence profile second evaluation, *ParLMSRBF-R* with uncertainty per product pathway

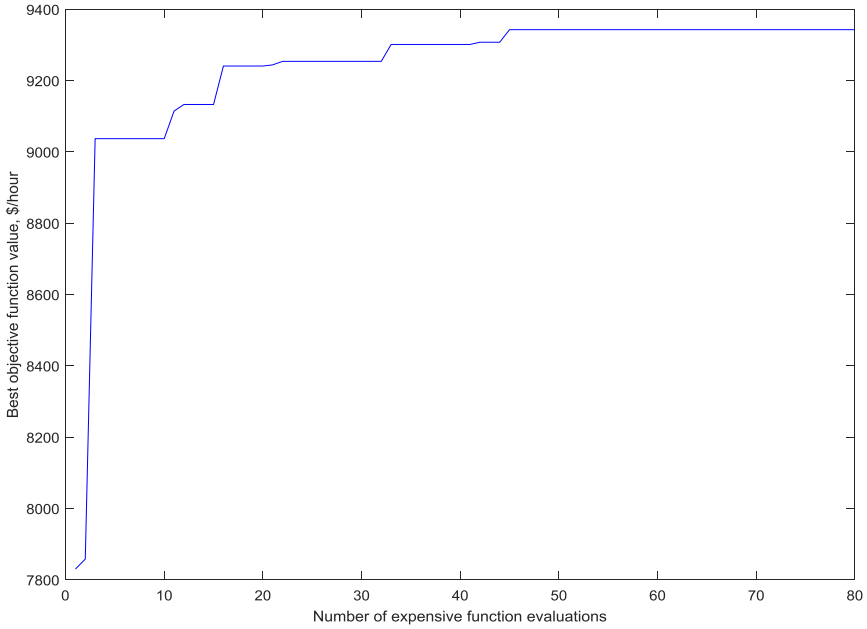

Figure 21: Convergence profile third evaluation, *ParLMSRBF-R* with uncertainty per product pathway

The first evaluation, presented in Figure 19, shows final convergence at the 71 expensive function simulation. In this evaluation, the algorithm restarts after the 48 expensive simulations once σ_n cannot reduce more and local optima is identified. This evaluation found its global optima after restarting the algorithm from scratch.

The second and third evaluation, Figure 20 and Figure 21, show convergence at the 65 and 45 expensive function simulation, respectively. For both evaluations, the algorithm does not restart, and parallel computing is used with $P = 2$ and $P = 4$, respectively. The third evaluation provides the operating conditions that will generate the highest profitability with uncertainty calculated per product pathway.

5.4 Case Study 2: Comparative analysis with Monte-Carlo (uncertainty calculated per product pathway)

For evaluating the method, the previously obtained points are contrasted with results from a Monte-Carlo simulation (MC), as mentioned before when uncertainty is simultaneously calculated the evaluation follows the procedure presented in Geraili et al. (2016). From 80 randomly selected points, the two ones that gave the best output results are selected and compared with the points obtained previously in *ParLMSRBF-R*. Table 6 presents the best five points. From these results, it can be noticed that when the uncertain parameters increase in bioethanol production, for overcoming this uncertain conditions the algorithm suggest to increase to the highest possible the temperature in simultaneous hydrolysis and cofermentation. Since there are less uncertain parameters in succinic acid production, the temperature of hydrolysis for succinic acid production shows its optima around 31 °C and enzyme loading ratio around 17 g enzyme/kg cellulose. This results are consistent for the three optima results obtained with *ParLMSRBF-R*.

Moreover, all the five points obtained, three from *ParLMSRBF-R* and two from MC simulation, are tested under the same uncertain conditions ($D = 100$). Table 7 presents the cash flow after tax results in which it is concluded that the best points for the hypothetical multi-product lignocellulose biorefinery are the operating conditions obtained in the third evaluation.

Table 6: Best operating points (uncertainty calculated per product pathway): *ParLMSRBF-R* and Monte-Carlo simulation

	Best operating points			
Scenario	T, hydrolisis for succinic acid, [°C]	Enzyme loading ratio [g enzime/ kg cellulose]	Sugar allocation (sugar to ethanol)	T, hydrolisis and cofermentation for ethanol, [°C]
Evaluation 1	31.19	17.49	0.200	53.00
Evaluation 2	30.26	17.61	0.200	53.00
Evaluation 3	30.60	16.30	0.200	53.00
MC (38)	33.83	16.57	0.237	46.21
MC (77)	31.84	16.18	0.251	47.26

Table 7: Biorefinery cash flow, $D = 100$ (uncertainty calculated per product pathway)

Scenario	Cash flow, USD/h		
	2.5^{th}	Mean	97.5^{th}
Evaluation 1	9252.90	9729.31	10205.73
Evaluation 2	9260.91	9731.22	10201.54
Evaluation 3	9276.87	9729.33	10181.78
MC (38)	9123.10	9588.86	10054.63
MC (77)	9120.05	9562.90	10005.75

When analyzing the outputs, it is noticed that their values are close from each other. Figure 22 & Figure 23 show a Kruskal-Wallis test of significance in which the best scenario is contrasted with the other ones. Both MC simulation points result to be significantly different from the best result and the results from *ParLMSRBF-R*. This analysis permits to conclude that the new global optimization method is better than MC simulation since its optima results are statistically

significant and better when uncertainty calculated per product pathway is simulated in the biorefinery.

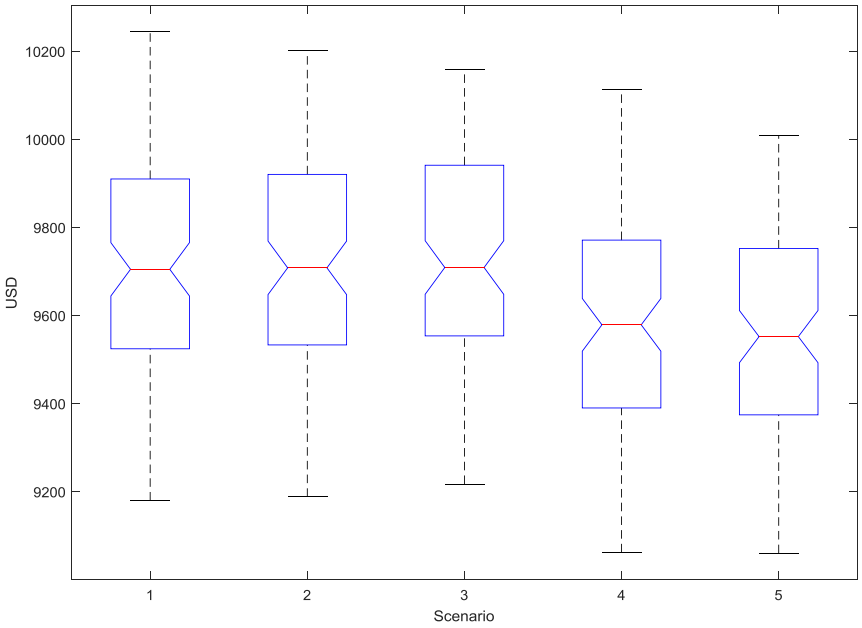

Figure 22: Kruskal-Wallis analysis for the best scenarios

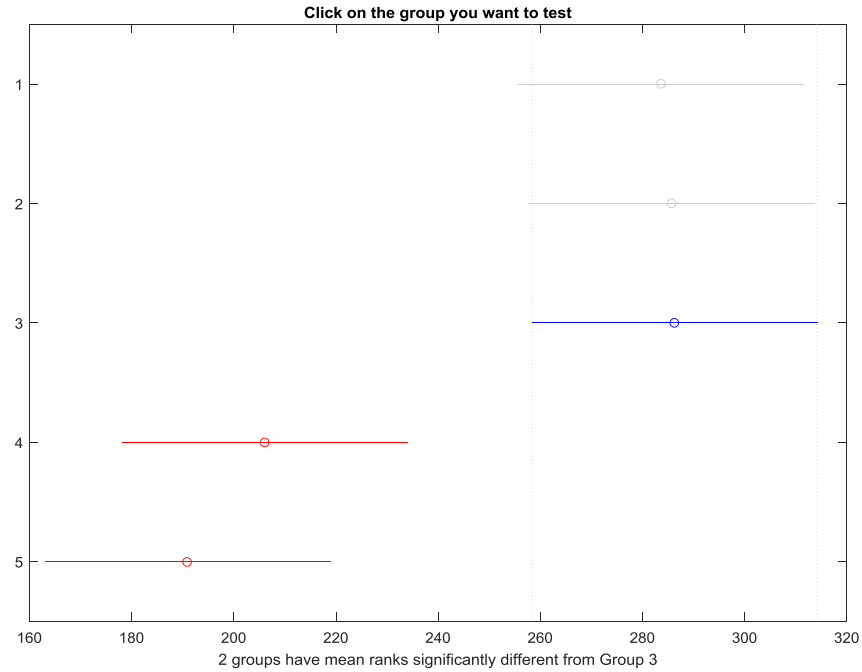

Figure 23: Statistical difference analysis for the best scenario (Scenario 3)

Finally, Table 8 presents the improvement obtained when using the points obtained with the *ParLMSRBF-R* method in contrast to the best point obtained from MC simulation. The results show that the implemented framework can improve in 1.69% the profitability in terms of the 2.5th percentile of cash flow after tax of the studied biorefinery in contrast with conventional methods, such as MC simulation, while reducing the quantity of expensive simulation required for optima convergence. The *ParLMSRBF-R* is highly competitive in terms of convergence since it obtains the optima result with less than a half of expensive simulations when compared with MC simulation. Moreover, the algorithm appears to require less expensive evaluations when the quantity of *P* evaluations increases.

Figure 24 shows a comparison between the best result obtained (Evaluation 3) with all the MC simulation's points evaluated. The three continuous lines represent the best scenario. This configuration considers technological risk minimization because the worst scenario is maximized, and as a consequence the mean and 97.5th percentile are pushed to better values. The normal distribution considers 95% of probability or 5% of significance. For this particular type of uncertainty (calculated per product pathway) the optima operating point is more conservative in terms of cash flow and in contrast with the previous evaluation.

Table 8: Scenarios results and improvement with respect the best Monte-Carlo points

Scenario	Cash flow, USD			Improvement			Convergence
	2.5th	Mean	97.5th	2.5th	Mean	97.5th	
Evaluation 1	9252.90	9729.31	10205.73	1.42%	1.46%	1.50%	Sim. 71
Evaluation 2	9260.91	9731.22	10201.54	1.51%	1.48%	1.46%	Sim. 65
Evaluation 3	9276.87	9729.33	10181.78	1.69%	1.46%	1.26%	Sim. 45
MC (38)	9123.10	9588.86	10054.63	-	-	-	after 80 sim.

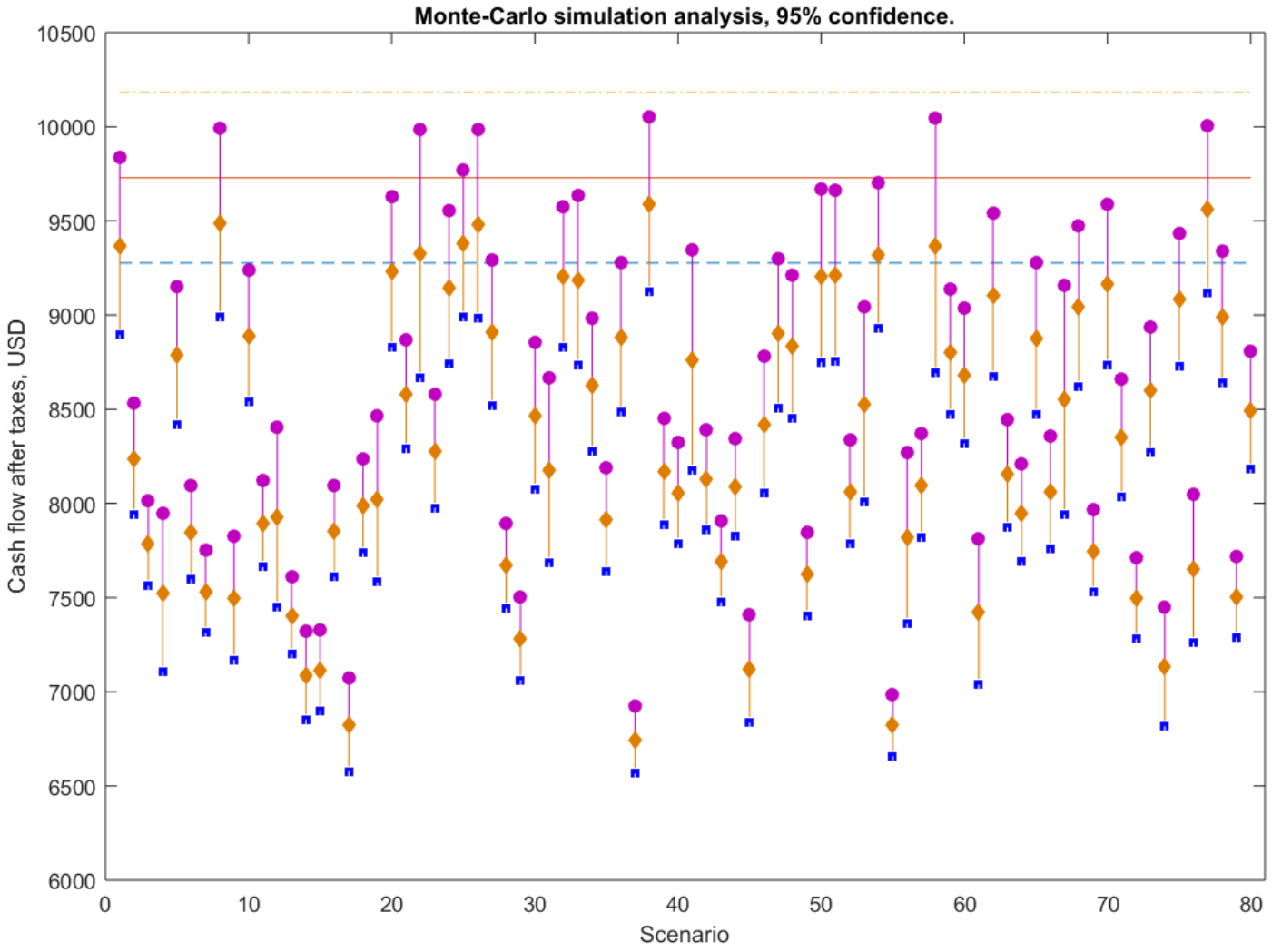

Figure 24: Comparative analysis between *ParLMSRBF-R* best scenario and Monte-Carlo method considering uncertainty per product pathway

6. CONCLUSIONS AND FUTURE WORK

The implemented optimization framework for renewable energy processes appears to be competitive with traditional procedures, e.g. Monte-Carlo simulation. The algorithm searches for the optimal operating conditions using a fitted and continuously updating Radial Basis Function without requiring to lose detail in the expensive simulation model. The algorithm selects candidate points to be evaluated near the current best solution neighborhood achieving exploration and exploitation in the solution domain. Moreover, uncertainties are explored with two different approaches, calculated simultaneously and per product pathway. Typically, the first approach is commonly used, but the second one aims to be more conservative in terms that the sensitive parameters come from each process unit allowing to consider each process independently. Table 9 presents the comparison of the number of parameters selected in each process section depending on the type of uncertainty. Clearly, the uncertainty calculated per product pathway has more parameters than when it is simultaneously calculated. Optimal conditions obtained with uncertainties calculated per product pathway intent to anticipate different conditions, not tested yet, that might influence the objective function and will be tested during optimization (after sensitivity analysis, see Figure 2).

Table 9: Number of uncertain parameters selected depending on the type of uncertainty

	Number of uncertain parameters selected		
Type of uncertainty	EHCF	SAEH	SACF
Simultaneously calculated	3	8	7
Calculated per product pathway	8	5	5

In terms of computational effort, the optimization algorithm employed requires less expensive function evaluations to reach global optima. In fact, *ParLMSRBF-R* finds optimal points after 54 expensive simulations when uncertainty is simultaneously calculated and after 45 when uncertainty is calculated per product pathway, both cases for the best scenario (Evaluation 3). Also, the improvement registered in contrast to the best value achieved with traditional methods, e.g., Monte-Carlo simulation, is 1.76% when uncertainty is simultaneously calculated and 1.69% when uncertainty is calculated per product pathway.

Table 10 presents the optimal operating conditions found when uncertainty is simultaneously calculated and when calculated per product pathway. The main difference is the temperature selected for enzymatic hydrolysis and enzyme loading ratio. Since the first type of uncertainty considers more parameters in succinic acid production, apparently for overcoming this condition the hydrolysis temperature raises. On the other hand, when less uncertain parameters from succinic acid production are introduced less temperature is required and more enzyme required. In the case of simultaneous hydrolysis and co-fermentation for ethanol production (EHCF) both cases suggest an increase of temperature from the previous one (48 °C) suggested from litterature (Geraili et al., 2015; Morales-Rodriguez et al., 2012) when uncertainty is introduced.

Table 10: Best operating conditions for both uncertain conditions

	Best operating conditions			
Type of uncertainty	T, hydrolisis for succinic acid, [°C]	Enzyme loading ratio, [g enzime/ kg cellulose]	Sugar allocation (sugar to ethanol)	T, hydrolisis and cofermentation for ethanol, [°C]
Simultaneously calculated	37.68	14.36	0.20	52.12
Calculated per product pathway	30.60	16.30	0.20	53.00

Finally, the new framework and optimization algorithm implemented increases the dimensionality of the original problem from *3-dimentional* to *4-dimentional,* which represents a substantial improvement for renewable energy production facilities and encourages to increase the produced products for evaluating technological risk.

For future work, the following ideas can be developed:

- Increase the quantity of added value chemicals, biofuels or both that a renewable energy enterprise has in its portfolio while evaluating technological uncertainty. Increase the dimensionality of the problem.
- Tune the *ParLMSRBF-R* algorithm's parameters and explore other types of RBFs for improving convergence towards optima.
- Evaluate the presented framework with other technological problems to evaluate its applicability in different businesses.

REFERENCES

Allaire, D., & Willcox, K. (2010). Surrogate Modelling for Uncertainty Assessment with Application to Aviation Environmental System Models. AIAA Journal, 48(8), 1791-1803.

Dale, B. E., & Holtzapple, M. (2015). The Need for Biofuels. (cover story). Chemical Engineering Progress, 111(3), 36.

Dal-Mas, M., Giarola, S., Zamboni, A., & Bezzo, F. (2011). Strategic design and investment capacity planning of the ethanol supply chain under price uncertainty. Biomass & Bioenergy, 35, 2059-2071.

Egea, J. A. (2008). New heuristics for global optimization of complex bioprocesses. PhD thesis, Universidade de Vigo, Spain.

Galperin, E., & Kansa, E. (2002). Application of global optimization and radial basis functions to numerical solutions of weakly singular volterra integral equations. Computers and Mathematics with Applications, 43, 491-499.

Geraili, A., & Romagnoli, J. A. (2015). A multi-objective optimization framework for design of integrated biorefineries under uncertainty. AIChE Journal, 61(10), 3208.

Geraili, A., Salas, S., & Romagnoli, J. A. (2016). A Decision Support Tool for Optimal Design of Integrated Biorefineries under Strategic and Operational Level Uncertainties. Industrial & Engineering Chemistry Research, 55, 1667-1676.

Geraili, A., Sharma, P., & Romagnoli, J. A. (2014). Technology analysis of integrated biorefineries through process simulation and hybrid optimization. Energy, 73, 145-159.

Gutmann, H. M. (2001). A radial basis function method for global optimization. Journal of Global Optimization, 19(3), 201-227.

Homma, T., & Saltelli, A. (1996). Importance measures in global sensitivity analysis of nonlinear models. Reliability Engineering and System Safety, 52, 1-17.

Humbird, D., Davis, R., Tao, L., Kinchin, C., Hsu, D., & Aden, A. (2011). Process Design and Economics for Biochemical Conversion of Lignocellulosic Biomass to Ethanol. National Renewable Energy Laboratory, Technical Report NREL/TP-5100-47764, Golden Colorado.

Kadam, K. L., Rydholm, E. C., & McMillan, J. D. (2004). Development and validation of a kinetic model for enzymatic saccharification of lignocellulosic biomass. Biotechnology Progress, 20, 698-705.

Kazemzadeh, N., & Hu, G. (2013). Optimization models for biorefinery supply chain network design under uncertainty. Journal of Renewable & Sustainable Energy, 5(5), 053125.

Kazi, F. K., (2010). Techno-Economic Analysis of Biochemical Scenarios for Production of Cellulosic Ethanol. National Renewable Energy Laboratory, Technical Report, NREL/TP-6A2-46588.

Keating, E. H., Doherty, J., Vrugt, J. A., & Kang, Q. (2010). Optimization and uncertainty assessment of strongly nonlinear groundwater models with high parameter dimensionality. Water Resources Research, 46(10).

Kim, J., Realff, M. J., & Lee, J. H. (2011). Optimal design and global sensitivity analysis of biomass supply chain networks for biofuels under uncertainty. Computers & Chemical Engineering, 35, 1738-1751.

Kokossis, A., Tsakalova, M., & Pyrgakis, K. (2015). Design of integrated biorefineries. Computers and Chemical Engineering, 81 (Special Issue: Selected papers from the 8th International Symposium on the Foundations of Computer-Aided Process Design (FOCAPD 2014), July 13-17, 2014, Cle Elum, Washington, USA), 40-56.

Kostin, A. M., Guillen-Gosalbez, G., Mele, F. D., Bagajewicz, M. J., & Jimenez, L. (2012). Design and planning of infrastructures for bioethanol and sugar production under demand uncertainty. Chemical Engineering Research & Design, 90, 359-376.

Leduc, S., Starfelt, F., Dotzauer, E., Kindermann, G., McCallum, I., Obersteiner, M., & Lundgren, J. (2010). Optimal location of lignocellulosic ethanol refineries with polygeneration in Sweden. Energy, 35, 2709-2716.

Martín, M., & Grossmann, I. E. (2011). Energy optimization of bioethanol production via gasification of switchgrass. AIChE Journal, 57(12), 3408.

Morales-Rodriguez, R., Meyer, A. S., Gernaey, K. V., & Sin, G. (2012). A framework for model-based optimization of bioprocesses under uncertainty: Lignocellulosic ethanol production case. Computers & Chemical Engineering, 42, 115-129.

Mugunthan, P., & Shoemaker, C. A. (2006). Assessing the impacts of parameter uncertainty for computationally expensive groundwater models. Water Resources Research, 42(10).

Powell, M.J.D. (1992). The theory of radial basis function approximation in 1990. In: Light, W. (ed.) Advances in Numerical Analysis: Wavelets, Subdivision Algorithms and Radial Basis Functions. Oxford University Press, Oxford, vol. 2, 105–210.

Razavi, S., Tolson, B. A., & Burn, D. H. (2012). Numerical assessment of metamodelling strategies in computationally intensive optimization. Environmental Modelling and Software, 34 (Emulation techniques for the reduction and sensitivity analysis of complex environmental models), 67-86.

Regis, R. G., & Shoemaker, C. A. (2004). Local function approximation in evolutionary algorithms for the optimization of costly functions. IEEE Transactions on Evolutionary Computation, 8 (5), 490-505.

Regis, R. G., & Shoemaker, C. A. (2007a). A stochastic radial basis function method for the global optimization of expensive functions. Informs Journal on Computing 19 (4), 497-509.

Regis, R. G., & Shoemaker, C. A. (2007b). Improved strategies for radial basis function methods for global optimization. Journal of Global Optimization 37 (1), 113-135.

Regis, R. G., & Shoemaker, C. A. (2009). Parallel stochastic global optimization using radial basis functions. Informs Journal on Computing 21 (3), 411-426.

Saltelli, A. (2002). Making best use of model evaluations to compute sensitivity indices. Computer Physics Communications, 145, 280-297.

Simpson, T., Poplinski, J., Koch, P. N., & Allen, J. (2001). Metamodels for Computer-based Engineering Design: Survey and recommendations. Engineering With Computers, 17(2), 129.

Sobol', I. M. (1993). Sensitivity estimates for nonlinear mathematical models. Mathematical Modelling and Computational Experiment, 1, 4, 407-14.

Song, H., Jang, S. H., Park, J. M., & Lee, S. Y. (2008). Modeling of batch fermentation kinetics for succinic acid production by Mannheimia succiniciproducens. Biochemical Engineering Journal, 40, 107-115.

U.S. Energy Information Administration. (2013). International Energy Outlook 2013 with projections to 2040.

Vlysidis, A., Binns, M., Webb, C., & Theodoropoulos, C. (2011). A techno-economic analysis of biodiesel biorefineries: Assessment of integrated designs for the co-production of fuels and chemicals. Energy, 36, 4671-4683.

Wang, G. G., & Shan, S. (2007). Review of Metamodeling Techniques in Support of Engineering Design Optimization. Journal of Mechanical Design, 129(4), 370-380.

Wu, Q. L., Cournede, P. H., & Mathieu, A. (2012). An efficient computational method for global sensitivity analysis and its application to tree growth modelling. Reliability Engineering and System Safety, 107, 35-43.

Zhang, J., Osmani, A., Awudu, I., & Gonela, V. (2013). An integrated optimization model for switchgrass-based bioethanol supply chain. Applied Energy, 102, 1205-1217.

Zhang, X., Srinivasan, R., & Van Liew, M. (2009). Approximating SWAT Model Using Artificial Neural Network and Support Vector Machine. Journal of the American Water Resources Association, (2).

Zondervan, E., Nawaz, M., de Haan, A. B., Woodley, J. M., & Gani, R. (2011). Optimal design of a multi-product biorefinery system. Computers & Chemical Engineering, 35, 1752-1766.

Zou, R., Lung, W., & Wu, J. (2009). Multiple-pattern parameter identification and uncertainty analysis approach for water quality modelling. Ecological Modelling, 220621-629.

APPENDIX: UNCERTAINTY INPUT IN BIO-KINETIC PARAMETERS

ID	Parameter	Units	Default value	Lower bound	Upper bound	Section of the process
1	α	-	1	0.8	1.2	EHCF
2	E_{1max}	g-protein/g-substrate	0.06	0.048	0.072	EHCF
3	E_{2max}	g-protein/g-substrate	0.01	0.008	0.012	EHCF
4	K_{1ad}	g-protein/g-substrate	0.4	0.32	0.48	EHCF
5	K_{2ad}	g-protein/g-substrate	0.1	0.08	0.12	EHCF
6	K_{1r}	g/(mg.h)	22.3	17.84	26.76	EHCF
7	K_{1IG2}	g/kg	0.015	0.012	0.018	EHCF
8	K_{1IG}	g/kg	0.1	0.08	0.12	EHCF
9	K_{1IXy}	g/kg	0.1	0.08	0.12	EHCF
10	K_{2r}	g/(mg.h)	7.18	5.744	8.616	EHCF
11	K_{2IG2}	g/kg	132	105.6	158.4	EHCF
12	K_{2IG}	g/kg	0.04	0.032	0.048	EHCF
13	K_{2IXy}	g/kg	0.2	0.16	0.24	EHCF
14	K_{3r}	h^{-1}	285.5	228.4	342.6	EHCF
15	K_{3M}	g/kg	24.3	19.44	29.16	EHCF
16	K_{3IG}	g/kg	3.9	3.12	4.68	EHCF
17	K_{3IXy}	g/kg	201	160.8	241.2	EHCF
18	E_a	cal/mol	-5540	-6648	-4432	EHCF
19	$\mu_{m,g}$	h^{-1}	0.31	0.2945	0.3255	EHCF
20	K_{4g}	g/kg	1.45	1.3775	1.5225	EHCF
21	K_{4Ig}	g/kg	200	190	210	EHCF
22	$C_{Etmax,g}$	g/kg	57.2	54.34	60.06	EHCF
23	$C_{Etx,g}$	g/kg	28.9	27.455	30.345	EHCF
24	$\mu_{m,xy}$	h^{-1}	0.1	0.095	0.105	EHCF
25	K_{5xy}	g/kg	4.91	4.6645	5.1555	EHCF
26	K_{5Ixy}	g/kg	600	570	630	EHCF
27	$C_{Etmax,xy}$	g/kg	56.3	53.485	59.115	EHCF
28	$C_{Etx,xy}$	g/kg	26.6	25.27	27.93	EHCF
29	α	-	0.65	0.6175	0.6825	EHCF
30	$qsmax,g$	g/(g.h)	10.9	10.355	11.445	EHCF
31	K_{7g}	g/L	6.32	6.004	6.636	EHCF
32	K_{7Isg}	g/L	186	176.7	195.3	EHCF
33	$C_{Etis,g}$	g/L	42.6	40.47	44.73	EHCF
34	$C_{Etmax,g}$	g/L	75.4	71.63	79.17	EHCF
35	$qsmax,xy$	g/(g.h)	3.27	3.1065	3.4335	EHCF
36	K_{8xy}	g/L	0.03	0.0285	0.0315	EHCF
37	K_{8Isxy}	g/L	600	570	630	EHCF
38	$C_{Etis,xy}$	g/L	53.1	50.445	55.755	EHCF
39	$C_{Etmaxsxy}$	g/L	81.2	77.14	85.26	EHCF
40	$qpmax,g$	g/(g.h)	5.12	4.864	5.376	EHCF
41	K_{9g}	g/L	6.32	6.004	6.636	EHCF
42	K_{9Ipg}	g/L	186	176.7	195.3	EHCF
43	$C_{Etip,g}$	g/L	42.6	40.47	44.73	EHCF

ID	Parameter	Units	Default value	Lower bound	Upper bound	Section of the process
44	$C_{Etimaxp,g}$	g/L	75.4	71.63	79.17	EHCF
45	$qpmax,xy$	g/(g.h)	1.59	1.5105	1.6695	EHCF
46	K_{10xy}	g/L	0.03	0.0285	0.0315	EHCF
47	K_{10Ipxy}	g/L	600	570	630	EHCF
48	$C_{Etip,xy}$	g/L	53.1	50.445	55.755	EHCF
49	$C_{Etmaxp,xy}$	g/L	81.2	77.14	85.26	EHCF
50	α_{sa}	-	1	0.8	1.2	SAEH
51	$E_{1max\ sa}$	g-protein/g-substrate	0.06	0.048	0.072	SAEH
52	$E_{2max\ sa}$	g-protein/g-substrate	0.01	0.008	0.012	SAEH
53	$K_{1ad\ sa}$	g-protein/g-substrate	0.4	0.32	0.48	SAEH
54	$K_{2ad\ sa}$	g-protein/g-substrate	0.1	0.08	0.12	SAEH
55	$K_{1r\ sa}$	g/(mg.h)	22.3	17.84	26.76	SAEH
56	$K_{1IG2\ sa}$	g/kg	0.015	0.012	0.018	SAEH
57	$K_{1IG\ sa}$	g/kg	0.1	0.08	0.12	SAEH
58	$K_{1IXy\ sa}$	g/kg	0.1	0.08	0.12	SAEH
59	$K_{2r\ sa}$	g/(mg.h)	7.18	5.744	8.616	SAEH
60	$K_{2IG2\ sa}$	g/kg	132	105.6	158.4	SAEH
61	$K_{2IG\ sa}$	g/kg	0.04	0.032	0.048	SAEH
62	$K_{2IXy\ sa}$	g/kg	0.2	0.16	0.24	SAEH
63	$K_{3r\ sa}$	h^{-1}	285.5	228.4	342.6	SAEH
64	$K_{3M\ sa}$	g/kg	24.3	19.44	29.16	SAEH
65	$K_{3IG\ sa}$	g/kg	3.9	3.12	4.68	SAEH
66	$K_{3IXy\ sa}$	g/kg	201	160.8	241.2	SAEH
67	$E_{a\ sa}$	cal/mol	-5540	-6648	-4432	SAEH
68	$\mu_{m,sg}$	h^{-1}	1.324	1.2578	1.3902	SACF
69	K_{Sg}	g/kg	1.123	1.0669	1.1792	SACF
70	K_{SIg}	g/kg	88.35	83.9325	92.7675	SACF
71	$P_{Crit,g}$	g/kg	17.23	16.3685	18.0915	SACF
72	i	-	1.3	1.235	1.365	SACF
73	K_d	h^{-1}	0.01	0.0095	0.0105	SACF
74	Y_i	g/g	0.765	0.7268	0.8033	SACF
75	Y_{SA}	g/g	1.31	1.2445	1.3755	SACF
76	Y_{AA}	g/g	0.999	0.9491	1.049	SACF
77	Y_{FA}	g/g	1.532	1.4554	1.6086	SACF
78	Y_{LA}	g/g	0.999	0.9491	1.049	SACF
79	msg	h^{-1}	0.061	0.058	0.0641	SACF
80	α_{SA}	-	0.626	0.5947	0.6573	SACF
81	β_{SA}	h^{-1}	0.355	0.3373	0.3728	SACF
82	α_{AA}	-	0.626	0.5947	0.6573	SACF
83	β_{AA}	h^{-1}	0.124	0.1178	0.1302	SACF
84	α_{FA}	-	0.665	0.6318	0.6983	SACF
85	β_{FA}	h^{-1}	0.105	0.0998	0.1103	SACF
86	β_{LA}	h^{-1}	0.21	0.1995	0.2205	SACF

VITA

Santiago Salas was born in Quito, Ecuador and received his Bachelor degree in Chemical Engineering from *Universidad Central del Ecuador* in 2012. In college, he was active in different student associations with different leadership roles, such as secretary of the Latin-American Chemical Engineering Students' Association, president of the Ecuadorian Chemical Engineering Students' Association, president of the *Universidad Central*'s Chemical Engineering Student Council, and founder and president of the AIChE-FIQ-UCE Student Chapter.

He started working for the Ecuadorian Oil & Gas industry as a technical assistant for the Facilities, Engineering, and Construction department at *Petroamazonas EP* for one year. Thereafter, he performed as a Process Engineer in *TECNA del Ecuador*. His work embraced conceptual, basic and detailed engineering for upstream and downstream Oil & Gas processes. In between and as a parenthesis, he attended to the course of History of European Civilization "*Notre Dame de la Clarière*" in Creutzwald, France. After one and a half years in the company, he moved back to *Petroamazonas EP* for working in the Project Management department as a Process Engineer. During the ten months he spent there, he collaborated in the conceptual and basic engineering of the Block 43 (ITT). The most challenging task accomplished was to formulate a methodology for characterizing the crude oil of the field. A significant desire of having new challenges motivated him to enter into a master's program. After being honored with a Fulbright scholarship, he started his graduate studies in the Cain Department of Chemical Engineering at Louisiana State University. He is currently a candidate for the Master of Science in Chemical Engineering to be awarded in May 2016 and plans to begin work on his doctorate upon graduation.